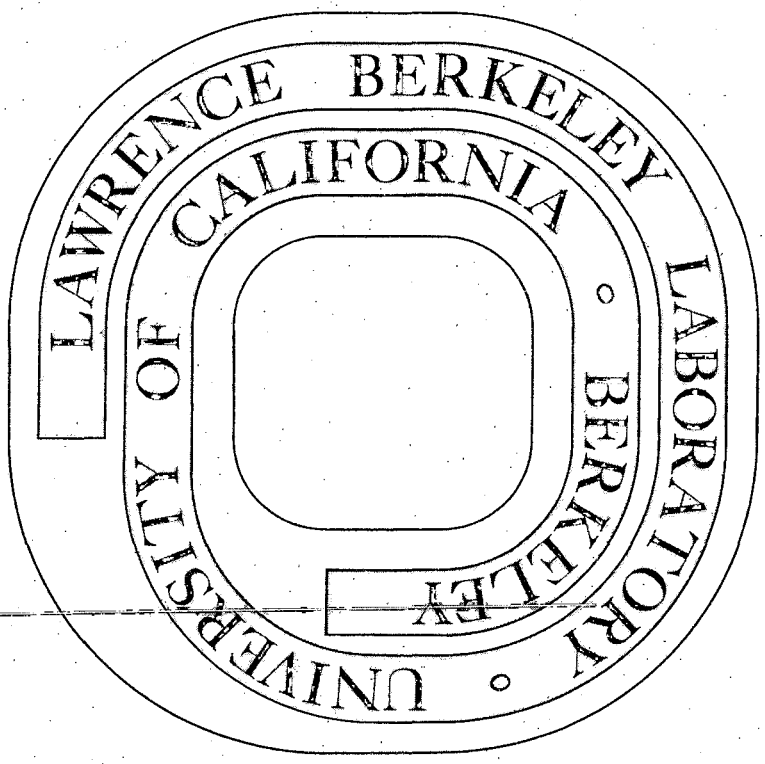

UCRL-10182
c.2

DISCLAIMER

University of California

Ernest O. Lawrence Radiation Laboratory

Berkeley, California

For publication in Advances
of Biology and Medical Physics
(Academic Press)

UCRL-10182

UNIVERSITY OF CALIFORNIA

Lawrence Radiation Laboratory
Berkeley, California

Contract No. W-7405-eng-48

HEAVY IONS AND SOME ASPECTS OF THEIR USE IN MOLECULAR AND CELLULAR RADIOBIOLOGY

Tor Brustad

April 1962

HEAVY IONS

AND

SOME ASPECTS OF THEIR USE

IN MOLECULAR AND CELLULAR RADIOBIOLOGY

by

Tor Brustad

Norsk Hydro's Institute for Cancer Research

The Norwegian Radium Hospital

Montebello, Oslo, Norway x)

x) The experimental part of the present work was carried out while the author was a guest of the University of California, Donner Laboratory of Biophysics and Medical Physics, under the auspices of the U.S. A.E.C. and the U.S. National Academy of Sciences.

ACKNOWLEDGMENTS

The author wishes to express his appreciation to Professor C. A. Tobias for the many stimulating discussions and for his continued support, which made the present work possible. It is furthermore a pleasure to acknowledge the untiring technical assistance of Messrs. P. Ariotti, T. Manney, G. Matley, and R. Adams.

The assistance of Dr. E. Hubbard and the HILAC crew and Dr. B. Jones and the 60-inch cyclotron crew is furthermore gratefully acknowledged.

Page

I. INTRODUCTION

When a biological system is exposed to ionising radiations numerous processes of unknown complexity are initiated, which eventually lead to the observed biological end-effect. From the earlier days of radiobiology it has been customary to distinguish at least three main stages in this long sequence of processes. The first stage lies in the general field of radiation physics. It calls for understanding of the quantity and manner by which energy is transferred to the biological system, including the spatial distribution of excited and ionised atoms and molecules - and the fluctuations of this distribution - at the instant after the exposure to the ionizing radiation. The next stage belongs to the general field of radiation chemistry, where the various types of radicals and molecular species, their yield and subsequent reactions with the biological system are subjected to investigations. The third stage lies in the field of biology, where the biological and physiological consequences are subjected to investigations, also including factors such as repair and recovery processes.

The detailed description of the problem of relative biological efficiency (RBE) for instance, would require the complete understanding of the various relevant processes in these fields. At the present time one is therefore forced to attempt to apply certain short-cuts such as to find correlations between some of the processes involved and certain criteria of the radiation damage. The present paper deals with the radiobiological consequences of one part of the first stage, namely the fact that the effect of ionizing radiation on a biological system not only

depends on the amount of energy absorbed, but also on the spatial distribution of that energy. Problems of this nature were investigated already many years ago; e.g. in studies of production of H_2O_2 by irradiation of gas free water, Fricke and Brownscombe (41) found X-rays unable to decompose water, whereas Neurnberger (66) obtained positive results with alpha rays.

The assumption has generally been made that the features of the ionized and excited molecules formed along the tracks of the ionizing particles are independent of the properties of the particles which produce them. The linear spacing between these events, however, depends on the charge state and velocity of the bombing particle. The linear spacing between ionizations produced in gases can be subjected to direct observations by Wilson's cloud chamber technique, and determination of the energy expenditure per ionisation can also be carried out in the gas phase by known physical means. Under these conditions, the number of ion pairs formed per unit track length can be determined experimentally, and is referred to as linear ion density or specific ionization. In solid and liquid state, as found in biological materials, determination of the specific ionization hinges on indirect means, namely by determining the ratio between the total energy absorbed per unit track length and the energy required to produce an ionisation in the material in question. As this latter quantity is not directly observable, it is generally assumed to be roughly equal to that of air. In this connection it should be noted that the concept of ionisation is used somewhat ambiguously, sometimes including, some-

times excluding excitations. Whenever the latter is the case, specific ionization will exclude the effects of excited molecules. In radiobiological applications this may be a serious oversimplification.

Considering these difficulties, Zirkle (114) suggested instead to discuss the distribution of physical events along the tracks in terms of the energy transferred, rather than of ion pairs formed, per unit track length. . He defined this quantity as linear energy transfer (LET). The LET is usually expressed in terms of electron volt per micron (ev/μ), or in the density independent units, such as ev $gm^{-1}cm^{2}$.

Two different methods have been used in order to obtain different LET-values experimentally. These are commonly referred to as the track segment method and the track-average method. The first method is used when monoenergetic particle beams are available. Thin samples relative to the particle penetration are exposed to a predetermined linear portion of the particle track, to which the desired LET pertains. Different LET values are obtained by utilizing different linear portions of the particle track in successive experiments, excepting the portions near the peak of the Bragg curve, where the doses delivered as well as the actual LET is difficult to evaluate. This method is commonly regarded as quite satisfactory, as it results in a relatively small spread of LET.

A refinement of this method has become possible within the last years, as accelerators have been built which produce monoenergetic beams of stripped nuclei up through atomic number 18, with energies of several Mev per atomic mass unit (amu)

(7, 103). With these types of particle beams, different LET's can be obtained by accelerating particles of different atomic number to equal velocity. This method has the advantage that the fraction of the total energy absorbed in a track segment which is dissipated as delta rays, remains constant, as does the shape of the delta rays spectra, irrespective of types of particles accelerated. This method is the most satisfactory at the present time, and will be discussed in more detail later.

The track average method on the other hand, was extensively used in the older investigations. It applies if the biological object in question is large compared to the length of the entire track of the particle, or if random portions of different tracks traverse the object. This results in a spread of LET values, ranging from that characteristic of the peak of the Bragg curve of the particle, to a minimum value determined by the charge and maximum velocity of the particle. The heterogeneity of the LET values becomes even more pronounced if there is a nonuniformity of the initial particle energy. Particularily this latter method led many investigators to the use of some kind of average LET.

Two different definitions of average LET have been commonly used, namely the track-average LET and the energy-average LET. Although more or less abbreviated methods have been used (15, 27, 28, 44, 58, 113, 117), in principles they may be defined as follows:

Assume the total number of particles, whose separate range is between R and R+dR to be N_R. The total track length

traversed by these particles in that range interval will be $N_R dR$. Let us furthermore assume that the LET corresponding to a particle range between R and R+dR is F' (LET). The track-average LET is then defined as:

$$\overline{LET}_{tr.av.} = \frac{\int_{R=0}^{R=R_{max}} F'(LET)\, N_R dR}{\int_{R=0}^{R=R_{max}} N_R dR} \qquad (1)$$

In analogy, let us assume the total number of particles whose separate kinetic energy is between T and T+dT, to be Q_T. The total energy dissipated by these particles in that energy interval will be $Q_T dT$. Let us furthermore assume that the LET corresponding to a particle energy between T and T+dT is F''(LET). The energy average LET is then defined as:

$$\overline{LET}_{en.av.} = \frac{\int_{T=0}^{T=T_{max}} F''(LET)\, Q_T dT}{\int_{T=0}^{T=T_{max}} Q_T dT} \qquad (2)$$

If different types of particles, a, b, c, etc. occur in the sample simoultaneously, the energy average LET would be calculated from the expression:

$$LET_{en.av.} = \frac{\left[\int_{T=0}^{T=T_{max}} F''(LET)Q_T dT\right]_a + \left[\int_{T'=0}^{T=T'_{max}} F''(LET)Q_T dT\right]_b \quad .....}{\left[\int_{T=0}^{T=T_{max}} Q_T dT\right]_a + \left[\int_{T=0}^{T=T'_{max}} Q_T dT\right]_b \quad .....} \qquad (3)$$

where each bracket refers to separate types of particles. A similar expression would be used for the track average LET of a mixed radiation field.

The concept of average LET has obvious shortcommings. Conger et al. (27) in a study of radiation induced chromosomal aberration in Tradescantia, found very different results depending on whether the energy-average or the track-average LET was used, which clearly shows the difficulty involved in the use of any type of average LET. In this connection it will be pertinent to note that a particle of low velocity and low charge can have the same LET as a particle of high velocity and high charge. The fast moving particle, however, will produce long ranged secondary electrons or delta rays, which will travel radically outside the track core of the particle, and produce further ionizations along their own tracks, which in spatial distribution resemble that of X-rays. The delta rays from the low velocity particle, on the other hand, will to a higher amount be confined to the track core of the particle. The question of whether the delta rays, radiobiologically speaking, are confined to the track core of the ion or not, can in the general case not be unequivocally answered, as it will depend on factors such as the size of more or less well defined "targets" as well as

distances over which indirect action of the ionizations occurs. Fluke and Forro (38) compared the efficiency of protons and alpha particles of identical LET to inactivate the plaque forming ability of T-1 bacteriophage, exposed in the dry state. Within the experimental error, no difference in efficiency was detected in this particular system. This finding does not exclude the possibility that a difference would have been found even for the same system, provided the comparison had been made between ions of higher charges.

From a fundamental radiobiological point of view there has been considerable interest in elucidation of the efficiency of different ionizing radiations to produce effects in biological materials. Studies of this nature have been useful in developing working hypotheses and theories for the mechanisms involved in the interaction between ionizing radiations and living systems; the target theory and radical migration theories are well known examples. No attempts will be made here to review the literature on the subject, as excellent introductions and discussions, both from a physical and biological point of view have been published (14, 15, 26, 30, 48, 58, 72, 90, 100, 112, 115, 116, 117). The development of the target-theory after 1946, for instance, has been reviewed by Sommermeyer (90).

The rapidly approaching space age has also provoked additional efforts in the study of radiobiological effects of different types of ionizing radiations, in attempts to elucidate the possible radiation hazzard in manned space travels (29, 79, 80, 81, 82, 101, 102).

Though a vast amount of work has been conducted to study

radiobiological effects of electromagnetic radiation, much less work has been done on effects of fast charged particles, and very little on ions heavier than alpha particles. The existence of high energy heavy ions in the primary cosmic radiation was discovered by Frier et al.(40) in 1948. They analyzed nuclear track emulsions exposed at high altitude and were able to identify tracks as being caused by fast charged ions up through atomic number 40. A great many investigations have since then been conducted in order to elucidate the physical characteristics of this component of the cosmic radiation. As rockets and satellites became available, an intensive study was started on the radiations in space and their radiobiological implications. As data are accumulating so rapidly in this field, reference is here made only to Physics and Medicine of the Atmosphere and Space, edited by Benson and Strughold (1960), which lists a good bibliography up to 1959-1960.

Attempts to obtain information on radiobiological effects of very densely ionizing radiations were probably first made by Tobias et al. (99), using fission fragments. Formidable problems are encountered in such studies, however, since both radiation doses and ionization densities are difficult to evaluate.

An important step forward was made when C^{+6}-ions were successfully accelerated in the Berkeley 60-inch cyclotron (3), and properties of these ions were studied by Tobias and Segrè (98). Subsequently beams of C^{+6}-ions were obtained in the same accelerator of sufficient intensity and stability (13) to permit a study of the radiosensitivity of haploid yeast cells (32). In 1957 the Heavy Ion Linear Accelerator

(HILAC) at the University of California (and some time later a sister machine at Yale University) became operative (7, 103). The HILAC is capable of producing a wide variety of beams of monoenergetic particles (10.4 ± 0.2 Mev/amu) up through atomic number 18 (45). The accelerator permits quick changes from one particle beam to another, which facilitates comparative studies of effects of different kinds of heavy ions on biological materials. The same experimental setup can be used for all heavy ion beams produced by the accelerator. This provides the additional advantage that some of the unavoidable errors involved in the dosimetry cancels out in experiments on the relative biological effectiveness (RBE).

The present paper describes some studies of the radiosensitivity of simple biological system as a function of the LET. In these experiments it was tried to keep biological and physical conditions as constant as possible, in order to facilitate mutual comparison when the LET was varied. Before an attempt is made to analyze the biological data, a discussion of the experimental setup and of the physical characteristics of the various radiations will be given.

II. PHYSICAL CHARACTERISTICS OF HEAVY ION BEAMS PRODUCED BY THE HILAC

A. The Experimental Setup.

The HILAC has been used successfully for accelerating beams of helium, boron, carbon, nitrogen, oxygen, fluorin, neon,

and argon to energies of 10.4 ± 0.2 Mev/amu (45). The beam is pulsed with an adjustable pulse repetition rate. However, in most of the investigations reported here, 10 and 15 pulses per second were used, with a pulse duration of 2 milliseconds. Means are available for varying the pulse duration, and in certain instances biological materials were exposed to a single pulse or a few pulses in succession. Average dose rates as low as a few rads per second and as high as 10^6 rads per second are available.

Fig. 1

Figure 1 shows diagramatically the experimental setup used throughout the present investigation. From the emit port of the accelerator the beam was first deflected by a strong "analyser magnet" and bent up to 30 deg. relative to the original beam direction, to ensure homogeneity of particle momenta. The beam then passed through the "monitor section" which contained some thin Al foils. These foils also served to scatter the beam sufficiently to furnish a homogeneous radiation field at the position of the biological samples at the very end of the apparatus.

Highest beam intensities were obtained when partially stripped ions were accelerated, such as D^{+4}, O^{+6}, O^{+5}, Ne^{+7}, and A^{+13}. Except A^{+13} these ions became completely stripped of electrons upon passage through the foils in the monitor section, and thus entered the "target section" as stripped ions. The target section consisted of an electrically insulated Faraday cup, made of 8-in. i.d. brass tubing with a removable vacuum tight back cover, which facilitated attachment of additional experimental equipment. As shown in Fig. 1, this cup, which is referred to as the "main Faraday chamber", was provided

with an extension into the beam pipe. The beam defining aperture was located just in front of the main Faraday chamber, and care was taken to prevent the beam from striking the extension of the latter. The beam defining aperture and the extension of the main Faraday chamber were both located within the magnetic field from a permanent magnet arranged perpendicular to the beam direction. This field served to prevent any electron present in the beam from entering the main Faraday chamber, and also to prevent secondary electrons produced inside the main Faraday chamber from scattering out of it.

The main Faraday chamber contained 3 absorber wheels, each with 9 Al foils of calibrated thickness and one blank hole to allow the beam to go through with full energy. This experimental arrangement, originally designed by Dr. Fluke, permitted a large number of independent absorber thicknesses to be placed in the beam path to degrade the particle energy. The main Faraday chamber also contained two sample wheels, each having 11 sample and 5 control positions, plus one blank hole to allow the beam to go through undegraded. All 5 wheels were turned by remote control from outside the target area. Precautions were taken in the design to make the leakage current from the chamber negligible.

Also shown in Fig. 1 is the "external Faraday cup" which could be kept electrically insulated from the main Faraday chamber. This cup was guarded by a magnetic field provided by two horseshoe magnets. The external Faraday cup could also be replaced by a thin Al or "Mylar" window, which allowed the beam to penetrate out of the apparatus, facilitating the alignment of the setup as well as the study of the flux homogeneity over the beam cross section.

B. Dosimetry of Heavy Ions.

1. Faraday Cups.

Having obtained a beam of homogeneous intensity distribution over the sample area, dosimetry was performed by measurement of the number (N) of bombarding particles per cm^2. Knowing this value and the total stopping power of the target material for the radiations in question, $(\frac{dE}{dx})$, expressed in units of Mev $gm^{-1}cm^2$, the dose in rads (D) was calculated as:

$$D = 1.602\ N(\frac{dE}{dx})\ 10^{-3} \qquad (1)$$

Measurement of the cross sectional area of the beam and of the flux distribution within that area, was performed in various ways:

1) at low beam intensity by densitometer readings of exposed DuPont safety film, type 1290.

2) at high beamintensity from the radiation induced colorization of "Czalid" paper. Beam areas determined from measurements of the diameter of the burn patterns obtained with the two techniques generally agreed to within a few per cent.

3) in some cases by nuclear track emulsions, mounted perpendicularly or nearly perpendicularly to the beam in the high vacuum of the main Faraday chamber, with subsequent counting of the flux density (and of track length, for determination of the energy spread of the ions). This technique was also useful for the additional purpose of testing the edge structure of the beam.

Fig. 2

Figure 2 shows the result of an analysis of the tracks produced in a nuclear track emulsion (Ilford, type k-2) exposed to C^{+6} ions.

a) shows the relative number of tracks counted per field of view illustrating a pronounced skewed flux distribution.

b) shows the relationship between number of tracks as a function of their range in the same emulsion. The ranges can be converted to energy equivalent units (Heckman et al. (45)), giving 117 Mev as the most probable energy of the C^{+6} ions at the sample position for this particular arrangement, i.e. after penetrating the Al foils in the monitor section only. The "full width at half maximum" corresponds to 1.5 Mev, which for the present type of the experiments is very satisfactory, particularly in view of the fact that the track-segment method was used throughout these investigations, without applying the low energy part of the Bragg curves of the heavy ions.

4) at different beam intensities by recording the beam current passing through a small aperture in the main Faraday chamber, relative to the beam monitors upstream. By moving the aperture, by remote control, across the beam cross section, a beam "profile" was obtained. The beam intensity, after passage through the aperture, was measured by using either the external Faraday chamber or the ionization chamber.

These different types of measurements showed the flux distribution across the beam area to be homogeneous to within a few per cent provided care was paid to proper alignment of the experimental setup. This conclusion was also borne out in

experiments employing biological test systems: It has for instance been shown that the remaining infectivity of dried T-1 bacteriophage depends in a strict exponential manner upon the absorbed dose (36). A skewed flux distribution over the sample area, however, would result in a deviation from this relationship, the more readily detected the lower the survival ratio tested. Whenever dose-effect curves were determined down to a survival ratio of 10^{-5}, this method was found as sensitive as any of the physical tests discussed above.

Knowing the beam area, the measurement of the doses in terms of number of bombarding particles per cm^2 was performed by integration of the beam current from the Faraday chambers, with a small correction for charge pickup of the ions, dependent upon the particle velocity (45). When samples were exposed on the sample wheels in the main Faraday chamber, the beam was stopped in the disks behind the samples. Consequently this chamber provided a direct measurement of the dose delivered to the samples.

For exposure of samples kept at various temperatures during the exposure, or when effects of various gases present during or after the exposure were to be tested, the experimental setup shown in Fig. 3 was used. In order to obtain different sample temperatures, the sample holder was designed as a hollow wheel, the interior of which could be flushed by a cooling medium or by circulating water from a thermostat regulated water bath. This chamber was also connected at the position shown occupied by the "external Faraday cup" in Fig. 1. The main Faraday reading remained unchanged with this chamber attached, whether the latter was kept at high vacuum as part of the

entire apparatus high vacuum, or separated by an aluminium or a "Mylar" window and kept in various gas atmospheres.

2. Ionization Chambers.

Particularly for exposure of biological samples to low doses, the need arose for a sensitive detector which could be calibrated independently of the Faraday cups, thus providing a check of the dosimetry already described. Some preliminary work was done with a thin film calorimeter (34), but the main effort was centered on the design and testing of ionisation chambers. The pulsed nature of the HILAC beam imposed certain restrictions on the design of the chambers, in addition to the problems involved as a result of the short penetration of the heavy ions (45, 68, 82). Based on Boag's analysis of ionization chamber characteristics (16), a design was arrived at which is diagrammed in Fig. 4. This parallel plate ionization chamber was usually operated with the sensitive volume of the chamber flushed with purified, dry N_2-gas, but for test purposes purified argon gas was also used.

Fig. 4

When the intensity distribution of the bombarding particles is homogeneous over the beam cross section, the dose at the position of the ionization chamber is given as (12):

$$D = \frac{Q\ W\ S_m'\ 10^5}{V\rho} \qquad (5)$$

where D is the dose in rads, ρ is the density of the gas in the chamber at the actual temperature and pressure, Q is the charge in columns collected from the collection volume V(cm^3)

of the chamber. W is the energy in ev per ion pair for the gas in the chamber, and S'_m is the mass-stopping power of the target material relative to that of the chamber gas. To determine the dose to the samples located a certain distance from the chamber, a correction factor must be applied which, under the present experimental conditions, is not significantly different from the Bragg ratio, if the energy of the particles in the actual sample is used to determine S'_m. Values of S'_m and W as functions of the heavy-ion energy were taken as equal to those of protons of the same velocity (12).

Fig. 5

Figure 5 shows some typical voltage saturation curves for an ionization chamber with a high-voltage collector spacing of only 0.82 mm., exposed to beams of C^{+6} ions of different average dose rates. Currents from ionization chambers, monitors, and Faraday cups were integrated with battery powered electrometers, and displayed on recorder charts. An electronic unit was designed and built which permitted automatic interception of the beam after delivery of a preset dose.

C. Particle Range and Stopping Power.

The experimental setup described permitted measurements of external Faraday cup readings relative to the monitor readings, as a function of the thickness of Al absorbers introduced into the beam path in the main Faraday chamber. These measurements provided determination of number-distance curves of the various ions accelerated. Figure 6 shows some examples of such measurements. The Ne-curve shows a pronounced slope, even for

Fig. 6

absorber thicknesses less than 30 mg./cm^2. This is partly caused by charge pickup of the ions as their velocity are reduced. After correcting for this effect by using data from Heckman et al.(45), such curves may be converted into general number-distance curves, from which for instance "mean range" values can be obtained. Ranges of some heavy ions, accelerated in the HILAC, are shown in Table I.

Table I

It can be seen from this table that the ranges of the heavy ions cannot be calculated directly from the Bethe-Bloch formula assuming completely stripped ions. This is not surprising, since the velocity of the ions is not much greater than that of the fastest electrons in the atoms of the absorber material. Furthermore, as the energy of the ions is reduced by the absorbers, the particle velocities approach that of their own K-electrons, resulting in a pronounced charge pickup. Both these effects tend to extend the range compared to that of the completely stripped ion. During the course of the present investigation, extensive studies of ranges and energy loss processes of heavy ions in emulsions (45) and in aluminium (68) were reported. Quantitative expressions were given for the ratio of the effective charge of the ions to their nuclear charge, as a function of the velocity of the different ions. When included in the range-energy formulas, agreement was found with experimental data also for other materials, as shown by Shambra et al. (82) in the case of mylar and polyethylene. Calculations of range-energy relations of heavy ions in any tissue composition could thus be performed, from which the stopping powers were derived. Table II serves to illustrate the ranges in and the stopping powers of a tissue equivalent

material (the composition of which was taken from Lea (58)), for some commonly used heavy ions of energy 10 Mev/amu. Table II

Except for protons and alpha particles, the ranges of the listed heavy ions are less than one millimeter, which limit the types of biological materials which conveniently can be studied.

If the external Faraday cup was replaced by an ionization chamber, the experimental setup permitted measurements of the ionization chamber response relative to that of the monitors, as a function of the thickness of the abosrbers introduced in the beam path in the main Faraday chamber. With the monitors calibrated against the Faraday cups, in terms of number of heavy ions per cm^2, such measurements could be expressed as total amount of energy dissipated per particle per unit track length, as a function of the remaining range of the particle in the material in question. Results of such studies are shown in Fig. 7 for 4 different heavy ions, after conversion to tissue equivalent material. Fig. 7 For low velocities of the heavy ions, the values of W and $S_m^{\prime}$ are not accurately known (12, 54, 93), which makes determination of the peak heights of the curves inaccurate. However, when plotted as shown in Fig. 7, the area under each curve must equal the total particle energy, which is known to be 10.4 ± 0.2 Mev/amu (45). This sets an upper limit to the peak height. The curves as drawn are based on the range-energy data discussed earlier, except for the peak regions. In the figure is also indicated the value of the integrated area under each curve, which in every cases is within the energy uncertainty of the various ions.

D. LET Distribution of Heavy Ions Penetrating Thin Samples.

For the detailed analysis of the dependence of biological effects on the spatial distribution of ionizations and excitations, the use of any averane LET would be expected to bee too crude, ~~as it is likely to be related to the ion density in a complicated way~~. Some authors have therefore proposed methods for calculation of the distribution of the entire family of electrons set in motion in the biological object. The application of such a method in the case of heavy ions will be discussed here.

When a heavy ion penetrates matter it will produce ionizations and excitations along its track. These may occur as single events or as clusters. A whole spectrum of electrons of all energies up to a characteristic maximum value will also be set in motion as the result of the primary interaction of the heavy ion with the absorbing medium. This spectrum is usually referred to as the initial or primary electron distribution. It can be calculated from Bohr's distribution law (10) :

$$dN = z^2 f \left(\frac{dT}{T^2}\right) \qquad (6)$$

where dN is the ralative number of electrons produced in the kinetic energy range T to (T+dT), and z is the effective charge of the heavy ion. The maximum kinetic energy which can be transferred to an electron is given by the expression:

$$T_{max} = 2m_o c^2 \left(\frac{\beta^2}{1 - \beta^2}\right) \qquad (7)$$

where β is the velocity of the heavy ion relative to that of light, and m_o is the rest mass of the electron.

From Eqs. (6) and (7) it can be concluded that the initial electron distribution is similar for all types of heavy ions of equal velocity. The only difference is that the actual number of delta rays per unit energy interval varies as z^2.

Some of the initial electrons will be set in motion with sufficient energy to create excitations and ionizations themselves along their own track, distinctly separate from that of the heavy ion. These electrons may produce secondary electrons, which again produce tertiary electrons and so on in a cascade type of a process, of which some clearly travel radially outside its parent track, whereas others do not. An unambiguous distinction between these two categories is not possible, and is in fact one of the serious shortcommings when the target theory is used for determinations of size and shape of "targets". Nevertheless, since electrons of different energies will create different ionization densities, a detailed analysis of the LET dependence of a biological effect will require a decision as to the amount of energy which will have to be transferred to an electron in order to form a separate track. Lea (58) analyzed this problem and concluded that energy transfers exceeding 100 ev generally should be regarded as separate spurs. Such transfers will be referred to as delta rays. With this definition of δ-rays, LET means the average energy dissipated per unit track length of the ionizing particle through all energy transfers (ionizations and excitations) whose separate energy contribution do not exceed 100 ev. For the

energy range of interest in the present discussion, LET can be calculated from the stopping power formula due to distant collisions, given by Bethe (8, 9) and recently refined by Sternheimer (96) :

$$\left(\frac{dT}{dx}\right)_{\gamma = 100\ ev} = \frac{2\pi n_o e^4}{m_o c^2 \beta^2} \left(\ln \frac{2 m_o c^2 \beta^2}{I^2(1-\beta^2)} - \beta^2 - \delta\right) \qquad (8)$$

n_o is the number of electrons per cm^3 of the absorbing medium. m_o is the rest mass of the electron, δ is Sternheimer's density correction, I is the mean excitational potential of the biological medium (66 ev) (12), e is the electronic charge and γ is the maximum energy transferred to an orbital electron and still counted as belonging to the track of the particle (γ = 100 ev).

In principle two methods are used for calculation of the entire LET-spectral distribution, where the "production of delta rays by delta rays" is included. The one method (28, 83, 92), which originates from Spencer and Fano's work (91), leads more readily towards a presentation of the data in terms of "differential track length" versus electron energy (from which the track average LET, referred to earlier, can be derived). The other approach, developed by Burch (23, 24) presents the data in terms of the amount of "local" energy ($Q_T \Delta T$) dissipated by the particles in differential kinetic energy intervals. (The energy average LET, referred to earlier, can be directly derived from this type of presentation). Both methods may be equally useful in radiobiological applications. In the present discussion, only the latter method will be used in calculation of the LET-energy spectra of some heavy ions of

different energy:

In order to take account quantitatively of the entire cascade production of delta rays, Burch suggested that the history of energy dissipation be followed in detail starting with the initial electron spectrum and using known cross sections for electron-electron interactions. In this way the total energy dissipated by electrons in kinetic energy intervals covering the entire spectrum may be arrived at. From such a "total energy dissipation spectrum" the relative amount of local energy ($C_T \Delta T$) is calculated, i.e. the relative amount of energy dissipated within the tracks of the electrons in the various kinetic energy ranges. This is done by multiplying the total amount of energy available within each energy interval by the ratio of stopping power of electrons where energy transfers (excitations and ionizations) up to 100 ev are counted only to the total stopping power of the electron. For the energy range of interest here this latter quantity can be calculated from the following equation, also derived by Bethe(10) :

$$\left(\frac{dT}{dx}\right)_{total} = \frac{2\pi n_o e^4}{m_o c^2 \beta^2} \left(\ln \frac{m_o c^2 E \beta^2}{2 I^2 (1-\beta^2)} - (2\sqrt{1-\beta^2} - 1 + \beta^2)\ln 2 \right.$$

$$\left. + (1-\beta^2) + \frac{1}{8}(1 - \sqrt{1-\beta^2})^2 \right) \qquad (9)$$

E is the relative kinetic energy of the electron, while the other parameters have been given earlier.

Equations (8) and (9) are both based on assumptions which do not hold for energies below a few kev, nor is any other theory

valid in this region. Considering these difficulties Burch (25) suggested to apply the range-energy measurements of low energy electrons in proteins, reported by Davis (31), to obtain LET values in the electron energy range up to 2.4 kev. The use of these experimental data results in considerably larger LET values than those which would have been derived from the theoretical formulas. This method is incorporated in the present work.

As the ionization density along the track core of a heavy ion may be very different from its accompanying delta rays, it is logical to regard the LET distribution of a heavy ion as consisting of two parts, that of its own track core and that due to the delta rays.

From stopping power formula of heavy ions (96) it can be concluded that the fraction of the total energy dissipated per unit track length by the heavy ion itself in energy transfers exceeding 100 ev (and consequently counted as delta rays) is equal for all ions of equal velocity. From this and the foregoing equations (6) and (7) it can be concluded that upon normalization of the LET-energy spectra to unit energy absorbed, all heavy ions of equal velocity will appear with identical delta ray spectra, whereas their track core LET's are different, namely proportional to z^2, where z is the effective charge of the ion. Depending on the velocity of the heavy ion, z may differ from the nuclear charge. Determination of the effective charge, however, can be carried out using the data of Heckman et al. (45).

Table III shows the result of calculations of LET-energy spectral distribution of the delta rays generated by heavy ions of energy 10 Mev/amu, 6.16 Mev/amu, 4.2 Mev/amu, and 3.3 Mev/amu.

Table III

In the present table the amount of energy dissipated in each delta ray spectrum is normalized to 1 rad.

Fig. 8
Fig. 9

In Figs. 8 and 9 are shown the total LET-energy spectral distributions for ions of H, He, B, C, O, and Ne, of energy 3.3 Mev/amu and 10 Mev/amu respectively, plotted according to a method suggested by Howard-Flanders (43). When plotted in this way the area under the curves between any two LET-values is equal to the amount of energy dissipated in that range. In the graphs presented the data are normalized so that the energy dissipated by the heavy ion track core plus its accompanying delta ray spectrum amounts to 1 rad. As the LET or the track core of each kind of heavy ions is single valued, the arbitrary width of the columns shown in Figs. 8 and 9 is determined exclusively for the purpose of graphical presentation, in order to be able to plot the amount of energy dissipated in the track core of the various heavy ions.

III. HYPOTETICAL MECHANISMS FOR RADIATION INJURY.

A. Method of Mathematical Description of LET Dependence.

Given the observed radiosensitivity, E(LET), for induction of a certain effect in a biological system, to different kinds of ionising radiations, for which the LET-energy spectra are known, one may derive a sensitivity function, P = f(LET), which describes the "true" LET dependence of the biological effect.

The relation between these functions may be described by the equation

$$E(LET) = \frac{k \sum_{T=0}^{T=T_{max}} f(LET)\, Q_T \Delta T}{\sum_{T=0}^{T=T_{max}} Q_T \Delta T} \qquad (10)$$

where k is a konstant, depending upon the effect studied, which will be referred to as the sensitivity constant.

Usually one will construct sensitivity functions based on certain hypotetical mechanisms for the radiation injury to the biological system. These are then fed into Eq. (10) to test the validity of the assumptions, according to the exclusion principle. Before discussing such hypotetical efficiency functions, certain aspects of the concept of radiosensitivity will be outlined, relevant in mutual comparisons of the efficiency for inducing certain effects by different radiations.

B. The Concept of Radiosensitivity.

In studies of radiation effects on cell populations it is usual to plot the fraction of cells surviving on a logarithmic scale against the delivered dose on a linear scale. Different shapes of such "survival curves" have been observed, depending on a variety of factors. It will be sufficient here to point out certain factors which are relevant when the effects of different types of ionising radiations on the same biological system are to be compared.

1. Exponential Dose-Effect Curves.

It has been shown for a number of biological systems that an exponential relationship exists between the fraction of cells surviving (S) and the dose (D) delivered:

$$S = e^{-\alpha D} \qquad (11)$$

The factor α, which determines the slope of the dose-effect curve represents a measure of the radiosensitivity of the particular effect under investigation. From Eq. (11), it is seen that

$$\alpha = 1/D_{37} \qquad (12)$$

where D_{37} is the dose corresponding to a survival ratio of 1/e. If the D_{37} is expressed in terms of number of bombarding particles per unit area, then α represents the sensitivity per bombarding particle, which commonly is referred to as the inactivation cross section (72). If the D_{37} is expressed in terms of the amount of energy absorbed, expressed for instance in rads, then α represents the sensitivity per unit energy absorbed.

The logaritmic dose-effect curve is often assumed to be the simplest relationship to interpret (35). It indicates that the injury to individual members of a homogeneous cell population is the result of the action of a single ionizing particle. However, a word of warning may be pertinent at this point:

Dittrich (33) has showed mathematically that it is possible

to combine 4 "two-hit" curves of different sized targets in such a way that by appropriate adjustments of the parameters, the resultant curve so closely resembles an exponential curve over many decades, that it would be difficult to distinguish experimentally from the latter. Zimmer (112) has recently reviewed the potentialities and limitations of target theoretical conclusions based on dose-effect curves.

In cases where logaritmic survival curves apply, the radiosensitivities of the biological system in question, to different ionizing radiations, are usually compared directly by using Eq. (12).

As far as the present author know, no case has been reported of change of a dose-effect curve from the exponential type for radiations of low LET towards the sigmoid type for radiations of high LET.

2. Sigmoid Dose-Effect Curves.

a. Shape of Survival Curves Independent of LET.

Most dose-effect curves are of the "sigmoid" type, with an initial flat portion indicating that no observable biological effect is produced until a certain amount of latent effect has accumulated. In many studies of the relative sensitivity of a biological system to different types of ionizing radiations it has been found that the shape of the survival curve remains approximately unchanged irrespective of the LET of the radiations studied. This was pointed out for instance by Tobias (100) in a study of inhibition of colony

formation of diploid yeast, exposed to 190 Mev deuterons, 200 kv X-rays, and to alpha particles. Under such conditions, the dose-effect curve observed for any radiation can be transferred into that for a standard or reference radiation, by multiplying the dose scale by a constant, characteristic for each type of radiation. Such constants are commonly referred to as dose reduction factors, using for instance the X-ray curve as reference. Under such conditions the relative radiosensitivity of the biological system to different ionizing radiations can be discussed in terms of dose reduction factors.

b. Shape of Survival Curves Dependent of LET.

As pointed out by Zirkle (117) it is a remarkable fact that in most systems, LET does not seem to affect the shape of the dose-effect curves. Experiments have been reported, however, where survival curves were found to be of the sigmoid type for radiation of low LET, but change shape and become truly exponential for radiations of sufficiently high LET. That the shape of the dose-effect curve can be a function of the LET was probably first demonstrated by Giles (43) in a study of chromosome aberrations of Tradescantia. Stapleton et al. (94) in a study of comparative lethal action of X-rays, protons, and alpha particles on dry spores of Aspergillus terreus, as tested by macroscopic colony formation, found exponential survival curves for protons and alphas, but a sigmoid dose-effect curve for X-rays.

Zirkle et al. (114) studied the inhibition of germ tube

formation of Aspergillus spores. They observed exponential dose-effect curves when using alpha rays with an LD_{50} of 19000 rep, whereas X-rays led to sigmoid survival curves with an LD_{50} of 125,000 r.

Recently, Hutchinson and Easter (52), using the Yale HILAC, studied two effects on Artemia eggs after exposure to 40 Mev He-ions and 160 Mev O-ions, and also to Co^{60} γ-rays. They showed very clearly that the pronounced sigmoid survival curve observed after exposure to Co^{60} γ-rays had a narrower "shoulder" in the case of He-ions, and that this was completely absent for O-ions, where a true exponential dose-effect curve was found. A similar trend has been found for the survival of the clone forming ability of mammalian cells (He La S3), by Deering (32). He found that X-rays and 40 Mev alpha particles resulted in almost identical sigmoid survival curves, with a 37% survival dose on the exponential portion of the curve corresponding to about 115 rads. For carbon ions and heavier ions of energy 10 Mev/amu, true exponential survival curves were found, with a 37% survival dose of about 100 rads for O-ions.

Whenever the shape of the dose-effect curve of a system changes shape if different radiations are used, it implies that different mechanisms are involved, whose relative importance are functions of the LET. Under such conditions comparisons of the relative radiosensitivity of a given biological system to different types of ionizing radiations cannot be expressed as a constant number since this will be dependent upon the survival level at which the comparison is made. The following

discussion will therefore consider only cases where the shape of the survival curves is independent of the LET of the radiations used.

C. The Track Segment Theory.

1. Introduction.

From the earliest days of radiation biology it has been postulated that there exist essential sites in the cells which must remain intact if the cell is to maintain its normal functions. A large number of investigations have been carried out where the induced effects are explained as being caused by two different mechanisms. One mechanism requires the presence of oxygen during irradiation in order to operate, the other does not. In the extensive investigations of Powers et al. (73, 74, 75, 76) on the radiation effects of dried spores of B. megatherium, where radiation induced radicals have much longer life times than in the wet state, it has been possible to sort out different types of reaction patterns. Both the oxygen dependent and the oxygen independent injury could be divided into sub groups, characterized by effects due to radicals of different life time, and studied by radical scavengers in gas form. To what extent similar reaction patterns occur in the wet state remains to be seen. In the following discussion the radiation injury will therefore be divided in the two main components only, the oxygen dependent and the oxygen independent.

A detailed discussion of the two mechanisms and their

energy requirements in terms of number of ionizations within a track segment of length "t" has been given by Howard-Flanders (48). In the following a brief review of some of the main points of his formulation will be included and attempts will be made to apply this type of mathematical formulation to describe the LET dependence of some biolgoical effects.

Howard-Flanders (48) distinguishes two types of radiation damaged essential molecules, denoted R' and R". The first one is without effect upon cell survival unless oxygen reacts with it. Upon reactions with oxygen he postulates that the latent injury is converted to a permanent and lethal form L_1 :

$$R' + O_2 \xrightarrow[\text{Rate } k_2(O_2)]{} \text{lethal injury } L_1. \qquad (13)$$

If the reaction with oxygen does not occur, the molecule will react in a different way and maintain its ability to carry out its biological functions :

$$R' \xrightarrow[\text{Rate } k_1]{} R_1 \quad (\text{No observed effect}). \qquad (14)$$

A second type of injury is postulated and denoted R", with the characteristics of being lethal whether oxygen is present or not :

$$R'' \longrightarrow \text{lethal injury } L_2 \qquad (15)$$

R" may be induced in many ways. Thus it is assumed that the interaction of two or more radicals may result in lethal

injury without radiation with oxygen.
Consequently R" may also be induced as a result of reactions such as

$$R' + \overset{\bullet}{OH} \longrightarrow R'' + H_2O \tag{16}$$

This implies that R" can be formed also partly at the expense of R'.

It is assumed likely that a single ionization will result in the formation of radicals which are reactive towards oxygen, whereas the interaction of two or more radicals may cause a change in the chemical structure without the intervention of oxygen. Combined with the fact that L_2 accounts for a larger fraction of the total injury caused by radiations of high LET, it is postulated that R' and R" can be produced by 1 and 2 ionizations respectively. For efficient production however, a larger number of ionizations may be required. Consequently Howard-Flanders postulated R' to be the result of 1 or more, but fewer than n ionizations within a track segment of length "t". R" on the other hand, was assumed to be the result of n or more ionizations within the same track segment.

From the LET-energy spectral distributions of the radiations in question, the mean number of ionizations per unit track length can be calculated for the radiations within the various energy intervals. Consequently, in order to put the track segment method outlined above into a useful mathematical frame work, i.e. in order to calculate the hypothetical probability for radiation injury as a function of the mean number of ionizations per unit track length, it will be necessary to :

a) Construct hypotetical probability functions for the probability of injury per unit energy absorbed, when the number of ionizations in "t" is just n (i.e. n and n only.

b) Calculate the probability per unit energy absorbed of obtaining just s (i.e. s and s only) ionizations in "t" when the mean number of ionizations in "t" is n.

These two problems will now be discussed separately.

2. Hypotetical Probability Functions for Radiation Injury.

Fig. 10

Figure 10 shows 3 different hypotetical probability functions, where P is the probability of injury per unit energy absorbed. The function denoted A was suggested by Howard-Flanders in an attempt to describe radiation induced injury to bacteria and yeast. For the oxygen dependent injury, P is assumed to be independent of the number of ionizations in the track segment "t" up to and including n-1. The oxygen independent component of the injury requires n or more ionizations, but P is otherwise independent of the number. Between n-1 and n is an arbitrary step shown, which makes the two mechanisms operate with different efficiency. There may be some justification for this, particularily in view of reactions of the type described by Eq. (16).

The probability function B was suggested by Howard-Flanders (personal communication) to be a more likely distribution. It represents a first order approximation, where

effect is assumed to be produced by single ionizations, with all ions equally effective up to a certain limit, where the higher order approximation takes over for the oxygen independent injury, in analogy to the distribution function A.

The probability function C is similar to B, except for the discontinuity between n-1 and n ionizations, similar to that of the distribution function A.

3. Probability for Certain Number of Ionizations in the Track Segment "t".

The problem of calculating the probability of a certain number of ionizations being formed within a given distance "t", when the mean number is m, has been discussed by several authors (35, 37, 48, 58, 59, 72). In such calculations, allowance must be made for both the statistical fluctuations of the number of ion clusters formed, and the frequency of ion clusters containing various numbers of ion pairs. Usually it is assumed that the statistical fluctuations of number of ion clusters formed follow a Poisson distribution. Furthermore, in the following calculation the same frequency distribution of the number of ionizations per ion cluster has been used as that applied by Howard-Flanders (48), which is based on the experimental data of Wilson (106) and Beckman (6). Table IV shows the result of calculations of the probability of n or more ionizations in the track segment "t" divided by the average number of ionizations in the same track segment (m). This quantity is referred to as P(n). Figure 11 presents these data in a graphical form.

From Table IV, by subtraction, one can calculate the probability of obtaining just n ionizations in "t" (i.e. s and s only) when the mean number is m. This quantity divided by m will in the following be referred to as P(s). The results of the calculation of P(s) as a function of m are shown in Table V and in Fig. 12.

Table V
Fig. 12

Combining the data from Tables IV and V with the probability function of Fig. 10, the hypotetical probability for radiation injury as a function of the mean number of ionizations per track segment of length "t", can be calculated. Such sensitivity functions were earlier (in Eq. (10), for brevity, referred to as f(LET).

Using the distribution function A in Fig. 10 one obtains the following sensitivity function:

$$f'(LET) = \left[P(s=1) + P(s=2) + P(s=3) \ldots + P(s=n-1)\right] \omega + P(n) \qquad (17$$

P(s) and P(n) is defined above, whereas ω allows the oxygen dependent and the oxygen independent mechanism to operate with different efficiency.

The distribution functions B and C in Fig. 10 result in the following sensitivity functions, with $\omega=1$, for the first one:

$$f''(LET) = P(u=n-1) = \left[\frac{1}{n}\left(P(s=1) + \frac{2}{n} P(s=2) \ldots\ldots\right.\right.$$

$$\left.\left.\frac{n-1}{n} P(s=n-1)\right]\right. \omega + P(n) \qquad (18)$$

This particular type of a sensitivity function P(u) will be

extensively used in the following discussions, especially with $\omega < 1$.

The relative biological efficiency (RBE) of a radiation A relative to that of a radiation B is obtained from Eq.(10) :

$$RBE = \frac{\sum_{0}^{T_{max}} (f(LET)\ Q_T \Delta T)_A}{\sum_{0}^{T_{max}} (f(LET)\ Q_T \Delta T)_B} \qquad (19)$$

In the following sections, attempts will be made to test predictions based on the theory outlined, against experimental data on virus, bacteria, yeast and enzymes.

IV. APPLICATION OF THE THEORY TO BIOLOGICAL SYSTEMS

A. Effects on Bacteriophages.

Inhibition of the Plaque Forming Ability of T-1 Bacteriophage Exposed in Dry State and in Nutrient Broth.

The efficiency of fast charged particles to inactivate dried T-1 bacteriophage as a function of the LET has been subjected to investigations by some authors (36, 37, 38, 39).

It was found that the amount of energy needed to inactivate the dried bacteriophage was nearly independent of the LET below about 400 Mev $gm^{-1}cm^2$, while more energy was required at higher LET values. This indicated that ionizations acted independently so long as their axial spacing was more than about 5 Å, or about 10 Å when allowance was made for the radial spread of the ionizations. These distances are much smaller than the diameter of the virus as judged from electron micrographs by Williams and Fraser (105) or even the dimension of the smallest sphere which could hold the amount of nucleic acid known to be contained in the T-1 bacteriophage (95).

In biological systems containing normal amounts of water, part of the inactivation may be due to "indirect" effects of radicals formed in the water, affecting the cell or the virus structures. Hutchinson (50) and Hutchinson and Nordcross (53), by comparing the radiosensitivity of certain enzymes irradiated in various cells either when dried or when normally hydrated, made estimates of the distances that radicals formed by ionizing radiation could diffuse in the cells. To make this estimate it was necessary to assume that the sensitivity of the enzyme was affected only by the ability of radicals formed within a certain distance to attack the enzymes in the cells.

The same question can be approached from a different angle by comparing the effectiveness of radiations of different LET and determining, in both wet and dry systems, the distance between ionizations beyond which they appear to act independently. Such a comparison has been made with T-1 bacteriophage, the result of which will be presented here. Samples of T-1, prepared from a filtered beef broth lysate, were exposed under

two conditions : a) In high vacuum, after prolonged vacuum drying. b) In nutrient broth suspension.

As criterium for radiation induced damage the loss of infectivity was used, estimated by the plaque count method. For exposure of T-1 in suspension 10/µl of the lysate of appropriate titer strength was put on glass cover slips, spread over an area of approximately 1 cm^2, covered by a 2 mg/cm^2 mylar film, and exposed to varying doses of heavy ions in moist air or in moist N_2-atmospheres. It should be remembered that no oxygen effect has been observed when T-1 is exposed in nutrient broth (46, 49, 62, 104). For the exposures of T-1 in dry state, aliquots of 50/µl of the virus lysate were dried on glass cover slips in a vacuum desiccator for 36 hrs. and then introduced into the high vacuum of the exposure chamber (Ca 10^{-5} mm Hg) and subjected to exposures of heavy ions. Under both conditions the samples were resuspended in nutrient broth immediately after exposure. The data on the radiosensitivity of dried T-1 were published and discussed in detail earlier (37).

Fig. 13

Figure 13 shows the result of these studies. The observed radiosensitivity is presented as the reciprocal of the 37% survival dose as a function of the LET of the various radiations used. Certain features of this diagram should be noted. At the highest LET studied the sensitivity in wet state is 2 - 3 times higher than in the dry state, whereas at low LET (i.e. about 20 Kev $\mu m^{-1} cm^2$) the corresponding sensitivity ratio is more than 6. Furthermore it can be seen from the graph that while the sensitivity in the dry state remains approximately constant over a considerable LET range, in the wet state the sensitivity is strongly LET dependent within the

same LET range. In fact the LET at which the sensitivity is reduced to 50% of its low LET value differs under the two conditions by a factor of about 5.5. This indicates that ionisations act independently in the dry state when separated by shorter distances than the wet state.

The solid curves in Fig. 13 are results of attempts to fit theoretical curves, based on the mathematical formulations previously discussed, to the observed radiosensitivities. As the radiosensitivity both in wet and dry state, within the entire LET studied, is decreasing with increasing LET, strong support is lent to the assumption that the inactivation can be produced by a single ionization in the right place. Although the mutual consistency of the dry state data is not sufficient to exclude the possibility of two ionisations as the minimum number for inactivation, the indication is strongly against 3 or more ionisations as the minimum number of ionisations required for inactivation (37). Both curves shown in Fig. 13 are therefore based on the assumption that the injury is the result of one or more ionisations within certain track intervals. This calls for applying the sensitivity function $f(LET) = P(n=1)$ when using Eq. (10) to fit theoretical curves to the experimental data. Table VI shows the parameters used in the theoretical analysis.

Dividing the sensitivity parameter pertaining to the wet state by that of the dry state, a ratio of 8 is obtained. The physical interpretation of this ratio is the following: If T-1 bacteriophages were exposed to a hypothetical radiation, with a single valued, infinitely small LET, the ratio of the sensitivity in wet state to that in dry state, would be predicted to be 8.

From inspection of Fig. 13 it is seen that a good correlation exists between the present theoretical curves and the experimental findings. Neglecting density differences in the two conditions studied, the present analysis indicates that the presence of nutrient broth increases the distances over which indirect action or energy transfer takes place by some 35 Å. These 35 Å represents an estimate of the distance over which radiation induced radicals or toxic products may exert a lethal action on the bacteriophage. It is interesting to note that it is quite consistent with diffusion lengths of radicals inside certain cells, as reported by Hutchinson et al. (50, 53) from a different type of analysis.

B. Effects on Bacteria.

Inhibition of Colony Formation of Shigella sonnei Exposed in N_2- and O_2-atmospheres.

A large number of investigations has been reported on the radiosensitivity of bacteria and the kinetics involved in the inactivation by ionizing radiations. However, rather few studies have been carried out on the LET dependence of the effects. Wyckoff (110) was probably the first one to carry out studies of this type. He investigated the inhibition of colony formation of E. coli exposed aerobically to X-rays of different filtration. Although a rather limited range of LET could be covered in this way, nevertheless he found the radiosensitivity to be declining with increasing LET. This

general finding was confirmed by Lea et al. (57) using β, γ, and X-rays and by Zirkle (119) who extended the LET range under investigation by using alpha rays. ~~(with the track segment method of analysis)~~

Experiments on inhibition of colony formation of the dysentery bacillus Shigella sonnei after exposure to neutrons and to X-rays under oxygenated and anoxic conditions have been reported by Howard-Flanders and Alper (47). As with E. coli a decreasing radiosensitivity was found with increasing LET in the presence of oxygen, whereas under anoxic conditions the data indicated an increase of the sensitivity when the LET was increased from that of X-rays to that of neutrons. Stimulated by this work, it was decided to carry out a detailed study of the radiosensitivity of Shigella sonnei (kindly supplied by Howard-Flanders) as a function of the LET of the inactivating radiations, and covering a wider range of LET than hitherto studied. In order to obtain more information about the amount of energy which is required locally for inactivation, it was decided to carry out the exposures in pure oxygen and in pure nitrogen atmospheres respectively.

The cells were grown in dilute nutrient broth suspension until the stationary phase was reached, centrifuged and washed 3 times in saline phosphate buffer (pH 7.6). Samples were prepared for irradiation from H_2- and O_2 pre-saturated saline phosphate buffered cell suspension, as single layers of bacteria on millipore filters. These filters were mounted on top of filter paper pads. Saline phosphate buffer was added to the pads in appropriate amounts. It soaked through the millipore filters, thus assuring a moist environment for the cells during bombardment. Samples prepared in this way have

certain very desirable features. By varying the moisture content of the supporting pad, the water layer on top of the cells can be adjusted to be so thin that negligible degradation of the heavy particle energies is caused in penetrating it. When flushing the bombardment chamber with O_2 gas or purified N_2 gas prior to and during irradiation, gas saturation in the cell layer was readily achieved, due to the free access to the flushing gases. This conclusion was also confirmed in some tests with a polarographic technique, utilizing a silver anode and a platinum cathode in a 0.1% sodium chloride solution. The ability of the cells to form colonies on nutrient agar was used as a criterium of cell survival. Under these conditions, Shigella sonnei shows a very reproducible, exponential relationship between the fraction of surviving cells and the dose of ionizing radiation.

Fig. 14 Figure 14 shows the results of these studies. The radiosensitivity is plotted as the reciprocal of the 37% survival dose, and expressed in rad^{-1}.

The sensitivity observed under anoxia shows an entirely different pattern from that found in the presence of O_2. Under anoxia a pronounced peak of the radiosensitivity appears, corresponding to a LET of about 300 Mev $gm^{-1}cm^2$. The sensitivity under aerobic conditions appears to be rather constant up to about 200 Mev $gm^{-1}cm^2$ and decreases rapidly with further increase of the LET. For radiation of low LET, the ratio of the sensitivity in O_2 to that in N_2 is about 2.7. For He-ions of LET about 90 Mev $gm^{-1}cm^2$ this ratio is reduced to about 1.7, and for Ne-ions with LET of about 3000 Mev $gm^{-1}cm^2$ it is about 1.25.

The finding of an oxygen effect even for as densely ionizing radiation as 130 Mev Ne-ions was at first rather puzzling. However, further tests showed that the magnitude of the O_2-effect at high LET depended more upon the velocity of the bombarding particle, rather than upon its actual LET. This is shown in Table VII.

Table VII

From Table VII it is seen that as the energy of the Ne-ions is reduced the O_2-effect decreases too, and for 1.9 Mev/amu Ne-ions the oxygen enhancement ratio is less than 1.1. Be-ions and C-ions with approximately the same energy per nucleon, but rather different LET result in equal oxygen enhancement ratio. These findings led one to conclude that under the present experimental conditions (also including such parameters as dose rate, pulsed nature of the radiations, etc.), no O_2-effect is associated with the densely ionized track core of the heaviest ions used in the present investigation. The observed O_2-effect for these radiations is due to the high energy delta rays which are energetic enough to travel out of the heavy ion track core.

Fig. 15

Figure 15 illustates the dependence of the oxygen enhancement ratio upon the energy per nucleon of He-ions (open circles). Shown is also the relationship between the energy per nucleon of the He-ions and the maximum energy, which these ions can transfer to delta rays (filled squares). A dotted line is drawn through the points, indicating that no oxygen effect would be expected for He-ions of energy less than about 1.5 Mev/amu, or a total energy of 6 Mev. Consequently there is no contradiction between the oxygen effect found for the present fast heavy ions and the old and well established

finding of no oxygen effect when Po alpha particles are used (58). It can therefore be concluded that the radiosensitivity observed with oxygen present during the exposure depends in a rather complicated way on qualities of the radiations used. To facilitate the mutual comparison and the detailed analysis of the radiosensitivity observed in oxygen atmosphere at different LET values, only ions of equal velocity should be used. This was not the case in the present investigation, and accounts partly for the scattering of the experimental points obtained under that condition.

Figure 14 also shows the result of attempts to fit theoretical curves based on the track segment theory outlined earlier to the observed data.

The LET dependence of the radiosensitivity observed under anoxic conditions has been calculated on the assumption that the injury is the result of 6 or more ionisations formed in a track segment of length $91\ \text{Å}/\rho$, where ρ is the numerical value of the density of the biological material in question. As seen from Fig. 14 the correlation is quite satisfactory.

The LET dependence of the radiosensitivity observed in the presence of oxygen has been calculated on two different assumptions : If use is made of the distribution function illustrated in Fig. 10 B, employing the sensitivity function calculated from Eq. (18), with $\omega = 1$, $u = 5$ and the same sensitivity parameter as used for the anoxic state, the dotted curve shown in Fig. 14 is found. The discrepancy between the curve and the experimental points rules out this probability function as a likely description of the mechanism involved. If, on the other hand, the distribution function illustrated

in Fig. 10 C is used, employing the sensitivity function calculated from Eq.(18) with $\omega = 0.63$ and $u = 5$ and the same sensitivity parameters as used to fit the anoxic data, the solid curve shown in Fig. 14 is obtained. In view of the dependence of the oxygen effect upon the velocity of the bombarding heavy ion, the fit is reasonable good, except for the highest LET values studied. It may be that for such high LET the linear distance between successive high energy delta rays is so short that an oxygen depletion will develop even beyond what is termed the track core of the heavy ion. The parameters used in the present track segment analysis of the radiosensitivity of Shigella sonnei are shown in Table VIII.

C. Effects on Yeast Cells.

1. Inhibition of Colony Formation of Haploid Saccharomycen cerevisiae after Exposure in H_2- and O_2-atmospheres, and Combined with Glycerol Dehydration.

In the history of radiobiology the emphasis in the interpretations has swung between giving the main importance to the direct or to the indirect effects of ionizing radiations. Effects observed on samples exposed in dry state and high vacuum have almost per definition been regarded as direct effects. Increasing the moisture content, on the other hand, has shifted the emphasis towards the indirect effects.

The observation that oxygen increases the radiosensitivity of cells, and the subsequent observation that it also affects

the sensitivity of dried biological material have been taken as additional evidence for the importance of the indirect effects. Although much of the controversy probably stems from lack of precise definitions, it has focused the attention upon these two types of mechanisms, the understanding of which is of fundamental importance for many aspects of radiobiology. The effects of oxygen and dehydration on the radiosensitivity of different biological systems have therefore been subjected to investigations. Wood (109) for instance, has reported on such experiments on yeast cells. Rosenberg (77) investigated the X-ray sensitivity of haploid yeast treated in hypertonic solutions to control the water content of the cells. He found that cells suspended in concentrated solutions (1 M to 6.9 M) of glycerol, glucose, ethanol, and methanol were less sensitive to inactivation by X-rays than those suspended in 1/15 M phosphate buffer. The degree of protection was found to be a function of the solute concentration, and in part or totally additive with the protection resulting from anoxia. Markovich (63) studied similar effects on E. coli K-12 (λ), using a variety of solutions.

A few years ago Sayeg et al. (78) carried out a study of the radiosensitivity of haploid yeast exposed aerobically to different radiations, including carbon ions accelerated in the 60-inch cyclotron at the University of California. With the availability of the great variety of radiations produced with the HILAC, it was decided to extend these studies and also to include the anoxic state. Further, it was thought useful to study the separate and combined effects of treatments with 6 M glycerol and anoxia on the radiosensitivity of haploid

Saccharomyces cerevisiae, as a function of the LET of the various radiations used. Preliminary results have been reported in abstracts (60, 61).

The cells were cultured on Potato Dextrose Agar (Difco) at room temperature for two weeks. The day prior to an experiment the cells were harvested, washed 3 times by centrifugation in 1/15 M KH_2PO_4 and suspended in the same buffer at a final concentration of 8.10^6 cells/ml. This suspension was kept on a wrist action shaker at room temperature until its use, and resulted in a cell population, uniform in radiosensitivity. There was no clumping and less than 0.1% of the cells were budding (108). The technique used for irradiation and gas equilibration were identical to those already described for Shigella sonnei. Immediately after irradiation the samples were resuspended in 0.5 ml. of 1/15 M KH_2PO_4 and spread on yeast-extract Dextrose Agar (Difco) in petri plates. After incubation for 24 hrs. at room temperature, survival was scored by microscopic counts of single cells and micro-colonies. Cells which were able to form micro-colonies of 10 or more cells were scored as viable. Tests showed that viability scored by this method gave the same radiosensitivity as that obtained by counting visible colonies.

Figure 16 shows the radiosensitivity as a function of the LET of the radiations used, for the different conditions under investigation. As seen from the graph no O_2 effect was found of any point of the entire LET range under investigation, when the cells were exposed in 6 M glycerol. Furthermore it was found that the glycerol treatment provided an additional pro-

tection compared to the anoxic level of cells exposed in the phosphate buffer also throughout the entire LET range. On the other hand, an oxygen effect was found when the cells were exposed in the phosphate buffer.

As seen from the figure the radiosensitivity under anoxic conditions increases with increasing LET up to about 700 Mev $gm^{-1}cm^2$ and decreases with further increase of the LET. This trend is similar to that found with Shigella sonnei, but the position of the peak on the LET scale is different. In the presence of oxygen, on the other hand, the response in yeast is quite different from that found in bacteria. For yeast a peak was observed at the same LET as that for the anoxic conditions, while in bacteria no peak was apparent at all.

Figure 16 shows the result of attempts to fit theoretical curves to the radiosensitivities observed under the different conditions, based on the track segment analysis.

The radiosensitivities of yeast cells exposed in 6 M glycerol both in the presence of oxygen and under anoxic conditions depend in the same way on the LET of the radiations. Under both conditions the LET dependence of the injury appears to be the result of 10 or more ionizations formed within a track segment of length 69 $Å/\rho$, with a sensitivity parameter, $k = 14. \times 10^{-4}$ rad^{-1}. The LET dependence of the radiosensitivity of cells exposed suspended in the phosphate buffer under anoxia also turned out to show the same general trend. It could therefore be fitted using the same sensitivity function, P(n=10), but the sensitivity parameter is higher by a factor of about 1.9.

The LET dependence of the radiosensitivity of the cells exposed in phosphate buffer in oxygen atmosphere is shown fitted on two different assumptions : If use is made of the distribution function illustrated in Fig. 10 B, employing the sensitivity function calculated from Eq.(18), with $\omega=1$, $u=9$, and the same sensitivity parameter as used for the anoxic state, the dotted curve shown in Fig. 16 is arrived at. As seen, this sensitivity function does not approach the general trend of the experimental findings, and consequently can be ruled out as a likely description of the mechanisms involved.

If, on the other hand, use is made of the distribution function from Fig. 10 C, with $\omega= 0.20$, $u=9$, and the same sensitivity parameter as used for the anoxic state, the solid curve shown in Fig. 16 is obtained. In view of the observation that the oxygen enhancement ratio also depends on the particle velocity, in addition to the actual LET, as discussed for bacteria, the fit is seen to be reasonably good. Table IX shows the parameters used in the present track segment analysis of the radiosensitivity of haploid yeast, for different conditions studied.

Table IX

In summary, the following points may be made: Yeast cells suspended in 6 M glycerol show no oxygen effect. Compared with the radiosensitivity of the cells exposed in phosphate buffer under anoxia, the glycerol treatment protects the cells by a factor of 1.9 throughout the LET range studied. A pronounced oxygen effect is found when the cells are exposed to radiation of low LET in phosphate buffer, an effect which decreases with increasing LET, but is observed even for fast Ne-ions. The LET response of the various effects studied can be described on the basis of the track segment analysis.

2. Induction of Dominant Lethals in Haploid Saccharomyces cerevisiae after Exposure in O_2-atmosphere.

In a study of diploid yeast zygotes formed by conjugation of one X-irradiated and one unirradiated haploid cell, Mortimer (64) was able to show typical signs of radiation damage of the zygotes, such as division delay, abnormal divisions, swelling, and death. He defined the damage responsible for inactivation of these half-irradiated zygotes operationally as dominant lethals. It was demonstrated that the induction of dominant lethals followed a sigmoid dose-effect relationship and furthermore that irradiation of the one haploid parent in a nitrogen atmosphere resulted in a twofold effective dose reduction in the zygote survival curve. It is noteworthy that this corresponds closely to the oxygen sensitization found for haploid yeast cell survival tested by inhibition of colony formation, as first investigated by Birge and Tobias (11), and discussed in more detail in the previous section. In a later investigation Owen and Mortimer (69) also reported on X-ray induced dominant lethals in diploid yeast cells. They found higher sensitivity for induction of diploid dominant lethals than that for the haploid dominant lethals, although haploid yeast cells are more radiosensitive than the diploid yeast.

It was decided to carry out a study of the LET dependence of induction of certain genetic effects of yeast, some results of which have been reported in abstract (65). In the present discussion only the result of a study of the LET dependence of induction of dominant lethals in haploid yeast will be presented. The present data of Adams, Brustad, and Mortimer

have not previously been published.

Cells of the haploid strain of Saccharomyces cerevisiae designated YO2022 were harvested from 24 hrs. old cultures on 2% yeast extract, 2% peptone, 1% dextrose, and 1% agar (YEPD) and resuspended in distilled water. Samples were prepared by putting aliquots of 50 µl on each of several specially cut non nutrive agar blocks. After exposure to various doses of heavy ions, irradiated cells were streaked along the surface of previously prepared YEPD agar blocks adhering to the surface of glass cover slips. Cells of the haploid strain YO2587a , harvested from 36 - 40 hrs. culture on YEPD and resuspended in distilled water were then streaked along the surface of the YEPD block, about 2 mm from the irradiated cells. This block was then inverted over an open end microdissection chamber in a micromanipulation stage. From 50 to 100 pairs were formed by placing in contact single cells from opposite streaks, using a glass microneedle to drag the cells to a center line. After 3 or 4 hrs. of incubation at 30° C, the paired cells were examined by microscope for zygote formation, and the position and appearence of the zygotes recorded. Examination of colony formation was performed at 12 hrs., 24 hrs., 48 hrs., 72 hrs., and 96 hrs. Zygotes producing colonies of 40 or more cells by 96 hrs. were counted as viable (64). The fraction of surviving zygotes was calculated and its dependence on the dose of the various radiations is shown in Fig. 17. It is seen that the dose-effect curves are not exponential. However, within the experimental errors, the shape of the dose-effect curves can be considered similar for all the radiations used. In other words, each dose-effect

curve can be converted into that obtained with any other radiation by multiplying its dose scale by a constant factor, characteristic for each type of radiations. In other words, the relative radiosensitivity can be discussed in terms of dose reduction factors, or as the reciprocal of the dose required for any pre-determined survival level. The latter method is used in Fig. 18, where the relative radiosensitivity is presented in terms of the reciprocal of the 37% survival dose, expressed in rad^{-1}.

Fig. 18

Comparison of Figs. 16 and 18 reveals that the radiosensitivity of haploid yeast cells as a function of the LET, shows the same general trend whether tested by the inhibition of colony formation (Fig. 16) or tested by induction of dominant lethals (Fig. 18). Unfortunately data for induction of dominant lethals as a function of exposure to different radiations under anoxic conditions were not obtained during these studies. Mortimer (64) has shown, however, that at least for X-radiation the oxygen enhancement ratio is equal for these two effects. In lack of more data for the anoxic state, one might guess that these too will show the same general trend as that for inhibition of colony formation under anoxia.

The solid curve shown in Fig. 18 is the result of a track segment analysis, which due to the factor mentioned above, is quite similar to that of inhibition of colony formation of haploid yeast. The curve for the radiosensitivity of the cells exposed in the presence of oxygen has been calculated employing the distribution function illustrated in Fig. 10 C, and Eq.(18) using $\omega = 0.20$ and $u = 9$, with a relative sensitivity constant $k = 34.4\ 10^{-5}\ rad^{-1}$.

The LET dependence of the induction of dominant lethals under anoxic conditions may thus be predicted to be the result of 10 or more ionizations in 40 Å/ρ, with the same relative sensitivity constant as already used for the oxygenated conditions. The present mathematical model would predict a twofold effective dose reduction in the zygote survival curve for exposure to radiations of low LET in a nitrogen atmosphere, consistent with the X-ray data of Mortimer (64). It will be interesting to compare the present predictions for the radiosensitivity under anoxic conditions over a wide range of LET when (or if) such data become available. The parameters used in the present track segment analysis of induction of dominant lethals in haploid yeast are shown in Table X.

D. Effects on Dried Enzymes.

1. Introduction.

Many investigations have been carried out on the radiosensitivity of dried enzymes, using X-rays, Co^{60}, gamma rays, protons, deuterons, and alpha particles, particularily by Lea et al.(58), and by Pollard et al.(72).

The present study was initiated in order to carry out a systematic study of the radiosensitivity of 3 different dried enzymes using radiations covering a much wider range of LET than emploied in earlier investigations. It was hoped that this large extension of the LET range used for the collection of inactivation data on 3 different enzymes would prove useful

in shedding some light on the mechanisms involved in the inactivating processes. The enzymes studied were lysozyme, trypsin, and DNase.

Dry enzyme samples (prepared from 2x crystallized material obtained from Worthington Biochemical Corporation and the Armour Laboratories) were prepared by pipetting known amounts of enzyme solution into bombardment disks (of steel, glass, plastic, cellophane or collodion films) and evaporating the solutions to dryness in a dessicator. After about 36 hrs. of drying at about 10^{-2} - 10^{-3} mm. Hg pressure, samples were transferred to the high vacuum (about 10^{-5} - 10^{-6} mm. Hg) of the bombardment chamber described earlier, and subjected to measured fluxes of heavy ions. After bombardment the samples were resuspended in appropriate buffers and tested for remaining enzymatic activity.

The DNase activity was determined from the rate of change of optical density at 260 mμ of a DNA-solution upon mixing with the enzyme, a method described by Kunitz (55).

The trypsin activity, if not otherwise specified, was determined spectrophotometrically from the rate of change of optical density at 253 mμ of a solution of N-benzoyl-L-arginine ethyl ester, upon mixing with the enzyme, as described by Schwert and Takenaka (84).

Lysozyme activity was determined from the rate of change of optical density at 450 mμ of a solution of Difco lysozyme substrate, when mixed with the enzyme, a modification of a method described by Shugar (83).

2. Efficiency per Unit Energy Absorbed.

Under the standard conditions used in the present investigation, exponential dose-effect curves were observed for all radiations used down to about 5% remaining enzymatic activity. Below this activity level, deviations from the exponential relationship were frequently observed, particularly in the case of lysozyme. This was partly due to the fact that radiation affected the solubility of the enzyme. However, no further discussion will be given here of these effects.

Figure 19 shows the radiosensitivity of the 3 enzymes, as a function of the LET of the radiation used, given as the reciprocal of the dose for 37% remaining enzymatic activity. It is seen that for all 3 enzymes the radiosensitivity decreases with increasing LET. If the LET increases, say from 30 Mev $gm^{-1}cm^2$ to 3000 Mev $gm^{-1}cm^2$ the radiosensitivity decreases to nearly 50% of its low LET value. This common trend supports the general idea that the inactivation can be caused by single ionizations properly placed.

A track segment analysis of the present enzyme data shows that quite satisfactory fits are obtained if one assumes the injury to be the result of one or more ionizations formed in a track segment of length approximately 10 $\text{Å}/\rho$. Thus, the theoretical curves shown in Fig. 19 have been calculated from Eq. (10), applying the sensitivity function f(LET) = P(n=1). Table XI shows the actual parameters used in the calculation.

3. Efficiency per Bombarding Particle.

As discussed earlier, analysis of inactivation data in terms of the efficiency for inactivation per bombarding particle ~~(instead of the efficiency per unit energy absorbed)~~ has frequently been used, and is commonly referred to as the inactivation cross section (72). It is determined from the exponential dose-effect relationship :

$$n/n_o = e^{-\sigma D}, \qquad (20)$$

where n/n_o is the fraction of the enzymatic activity remaining after a dose of D particles/cm^2 have been delivered to the sample. σ is the radiation inactivation cross section. The studies by Lea (58) and by Pollard et al. (72) led to the general conclusion that an enzyme molecule is inactivated whenever a primary ionization occurs inside the molecule, whereas ionizations occurring outside the molecule as well as excitations may be regarded as ineffective in the inactivation processes. On these assumptions the relationship between the inactivation cross section and the ionization density of the radiations used was reported to be (72) :

$$\sigma = \sigma_o (1 - e^{-iL}), \qquad (21)$$

where i is the mean number of primary ionizations per unit length and L is the average thickness of the enzyme molecule, σ_o, the inactivation cross section corresponding to infinitely high LET, should therefore equal the geometrical cross section of the "target", which, for enzymes in general was reported to

be the entire molecule. By using radiations of different LET, determination of both size and shape have been reported by many authors. One of the difficulties met in conducting such studies has been the lack of suitable sources of radiations with high and simoultaneously well defined LET, which are necessary for determination of T_o. The present inactivation data covered a very wide range of LET and consequently lent themselves for analysis according to this theory.

One of the implicit assumptions of Eq.(21) is that the diameter of the track of the bombarding particle is small compared to the diameter of the "target" to be determined. This problem has been discussed by Pollard et al.(72) and found to be reasonably true of the primary events caused directly by the ionizing particle and for those secondary electrons whose energy do not exceed certain threshold values. Secondary electrons of energy exceeding this threshold value can produce ionizations and consequently inactivations at considerable distances from the track core of the bombarding particle. The effects of these delta rays will have to be added to that calculated from Eq.(21) in order to compare the values derived by means of this theory with the directly observed inactivation data. Delta ray corrections appropriate for this type of analysis was first developed by Lea (58) for radiations of relatively low LET and recently extended by Dolphin and Hutchinson (34) to include very densely ionizing radiations. In a critical review of Lea's delta ray correction and the many inaccurately known parameters involved in it, Pollard et al.(72) conclude that Lea's delta ray correction is likely to be "an overestimation by a factor of 2 and probably more".

Fig. 20

Figure 20 shows the inactivation cross sections of the 3 enzymes studied, plotted as a function of the total stopping power $(\frac{dE}{dx})$ of the target material for the various radiations used. It is seen that per bombarding particle a Ne-ion of total stopping power about 4500 Mev $gm^{-1}cm^2$ is more than 65 times as effective as a proton of total stopping power about 40 Mev $gm^{-1}cm^2$. In fact, the inactivation cross sections of the 3 different enzyme molecules at the highest ionization densities used in the present investigation, are about 15 times larger than their expected geometrical cross sections, as determined from other physico-chemical methods. One is therefore forced to conclude that provided the simple one hit target theory briefly outlined above, applies to these dry enzyme systems, a rather drastic delta ray effect will have to be invoked in order to bring the theoretical predictions based on Eq.(21) into accord with the present experimental data. For instance, it will be necessary to assume that 93% of the observed inactivation cross sections at the highest LET studied in the present investigation, is due to delta rays, in order to bring these data into accord with known molecular dimensions. Even if all the assumptions involved in the simple target theory formulation outlined were valid, any determination of a target size by using heavy ions is bound to be highly uncertain in view of the very large and simultaneously very uncertain delta ray correction on top of a 10% error of the experimental data, which is reasonable in this type of experiments.

Fig. 21

Figure 21 shows the results of attempts to fit theoretical curves (dotted) based on the simple one-hit target theory

outlined, to the present inactivation data. In order to perform these calculations, "targets" of different molecular weights were assumed. The effects of delta rays were calculated according to the method suggested by Dolphin and Hutchinson (34), and are included in the theoretical curves. The solid curves shown are best fits through the experimental points.

Target sizes chosen so as to make satisfactory fit with the experimental points in the range above 1000 Mev $gm^{-1}cm^2$, corresponds to molecular weights larger than those determined from other physico-chemical methods, as shown in Table XII.

Table XII

As already mentioned, it is believed that the assumptions underlying the delta ray correction used in calculation of the curves of Fig. 21 will result in an overestimation of the correction (72). It therefore seems justified to conclude that the "radiation" molecular weights given in Table XII rather represent the minimum sizes compatible with the theory. Consequently, the present analysis of the efficiency of different heavy ions to inactivate dried enzymes appears to result in larger "target" sizes than the known molecular dimensions, at least of the order shown in Table XII. Whatever the reason or reasons for this may be, it seems logical that the following factors may contribute to the discrepancy :

1) An enzyme molecule "hit" by a heavy ion may be unable to retain all the energy dissipated in it, and under appropriate conditions transfers sufficient energy to neighbouring molecules to inactivate them also. A plausible mechanism for such energy transfer could simply be heat conduction, as the temperature along the track of a very densely ionizing particle is likely to be quite high. A deeper insight into the actual

mechanisms involved may be obtained by exposing samples at different temperatures to various heavy ions with successive analysis of Arrhenius plots. Some preliminary data are available (19, 20) and a more detailed study is planned.

2) The diameter of the heavy ion track core is not sufficiently small compared to that of the enzyme molecules.

3) The passage of a heavy ion sufficiently near an enzyme molecule may transfer enough excitation energy to the molecule to inactivate it, without the simoultaneous occurrence of an ionization, a mechanism which one may expect to become more likely the higher the LET of the radiation (70).

In spite of all the uncertainties involved in the present type of analysis, at least it demonstrates that quite a large fraction of the observed effect is due to delta rays, when use is made of fast, heavy ions.

Given the molecular weight of the target molecule, one can deduce empirically the correction required to obtain a reasonable correlation between the ionization density along the track core of the radiations used and the molecular dimensions according to Eq.(21). The introduction of a correction of this required magnitude, however, would call for additional assumptions on top of the many already involved.

For these reasons it is the opinion of the present author that the use of heavy ions in this type of experiments are quite illusoric as tools for determination of target shapes and very unreliable for determination of target sizes.

E. Factors Modifying the Radiosensitivity of Dried Enzymes.

1. Effects of Admixtures of Foreign Substances.

The analysis of the inactivation data of heavy ions, discussed above suggested larger radiation target sizes than the known dimensions of the enzyme molecules. This may be interpreted to mean that under certain conditions intermolecular energy transfer processes are of importance in radiation inactivation of proteins exposed in the dry state, as is well known to be the case when proteins in solutions are exposed. This interpretation is not new. Alexander and Charlesby (1) have demonstrated protection against direct action of ionizing radiation on polymers, when aromatic rings are attached to the main chain of the polymer molecule. Evidence for molecular interactions (energy transfer) in X-irradiated solids has been reported by Norman and Ginoza (67). They also found that the radiation resistance of catalase was increased by the addition of glutathione. Braams et al.(17) and Braams (18) found variations of the radiosensitivty of dry enzymes with admixtures of some inert materials. The present author has studied effects of various inert, foreign substances, on the radiosensitivity of trypsin and lysozyme, exposed in the dry state. Pronounced changes of the radiosensitivity were observed even after exposure to very densely ionising radiations, such as C^{+6}-ions (19, 20).

If molecular energy interactions play a role in radiation inactivation of dry enzymes, it would be expected that different kinds of molecules when mixed with the enzyme would display different efficiencies for interferring with the energy migration

patterns. In other words, it should conceivably be possible to find types of foreign molecules which, when mixed with the enzymes, could cause one of the following interactions:

a) increase the radiosensitivity of the enzyme,

b) decrease the sensitivity of the enzyme,

c) not interfere with the radiosensitivity of the enzymes.

Fig. 22

Figure 22 shows the effect of some compounds, chosen only to illustrate the 3 patterns referred to above for the particular case of trypsin exposed to 115 Mev carbon ions. The inactivation cross section is plotted as a function of the relative concentration of the foreign molecules in mixture with the enzyme. It was found for instance that ribose, lactose and raffinose all increased the radiosensitivity of trypsin, and on a molar basis proved to be approximately equally effective. Figure 22 presents the results obtained using ribose, illustrating the first type of interaction (Type a), mentioned above.

In experiments using dextran molecules of known molecular weight averages, a similar relationship was found to apply also for these large molecules, but on a molar basis they were more effective than the sugars discusses earlier. This is also shown in Fig. 22.

As an example of an interaction of the second type (Type b), is shown the effect of admixtures of the cyanine dye, pinacyanole ($C_{25}H_{25}N_2$ I), which is known for its use as a red sensitizer in photographic emulsions. As shown in the graph, pinacyanole decreased the radiosensitivity of trypsin, and thus protected the enzyme against radiation injury. After

admixtures of the highest concentrations of ribose and of pinacyanole used in the present investigation, the respective inactivation cross sections of trypsin differed by more than a factor of 6, corresponding to target volumes differing by a factor of almost 15.

As an example of an interaction of the third type (Type c), i Fig. 22 is shown the inactivation cross section of trypsin as a function of the concentration of cysteine (HCl). Under the conditions used in this experiment, no pronounced protecting or sensitizing effect was found. Preliminary experiments indicated, however, that while cysteine did not protect the pure enzyme against radiation injury resulting from densely ionizing radiation, it did appear to be able to prevent the enhancement of the radiosensitivity by the various sugars. However, because of certain difficulties during the exposure of the experiments with cysteine, this result is somewhat questionable. Thus, Butler and Robins (21) using X-rays and a different assay technique, found cysteine to protect by a factor of 4 (M = 35), and Braams (18), using deuterons found a protection of 1.8 in the case of invertase.

These studies of effects of various admixtures, show clearly that the radiosensitivity of dry enzymes can be greatly modified, to values either larger or smaller than those observed for the pure enzymes. It shows that a primary ionisation <u>outside</u> the enzyme molecule is not necessarily ineffective, nor is it necessarily 100% effective if occurring inside the enzyme molecule. It appears that under certain conditions, such as after exposure to densely ionizing radiations, intermolecular energy transfer processes may also be

of importance in radiation inactivation of biological materials. Under the present conditions these processes appeared to be of a rather non-specific nature, and high concentrations of the foreign molecules had to be used to uncover the effects. It does not seem unreasonable to assume that conduction of heat from the very densely ionized track of the heavy ion is an important contributing factor in this process.

2. Effects of Temperature during Irradiation.

That the temperature of dried enzyme samples during the exposure to ionizing radiations markedly influences the inactivation processes, was shown by Setlow (85) and by Pollard et al. (71). Setlow studied the radiosensitivity of dried samples of catalase exposed to deuterons and photons (λ = 2537 Å) as a function of the temperature of the samples during the exposure. When exposed to deuterons, the inactivation cross section was found to increase with increasing temperature, going through 3 different plateaus. This was taken to mean that at low temperatures one quarter of the molecule was inactivated, at intermediate temperatures one half of the molecule was inactivated, and at high temperatures, below 370° K, the whole molecule was inactivated by one primary ionization. At even higher temperatures, inactivation cross sections larger than that of the geometrical dimension of the molecule were found. The effect was suggested to arise either from excitations due to the passing particle, which at temperatures so close to thermal inactivation might be sufficient for inactivation, or it could arise from an indirect effect on the catalase molecule by the surrounding materials. When catalase

was exposed to deuterons at room temperature, the radiosensitivity was found to be more than 1.5 times higher than that observed at liquid nitrogen temperature. For photon exposure (λ = 2537 Å) the corresponding ratio was found to be about 3.8.

In a study of the radiosensitivity of trypsin exposed at various temperatures to C-ions, the present author found a small difference between the radiosensitivity at room temperature compared to that observed at liquid nitrogen temperature (39). A similar response was also found in the case of lysozyme exposed to oxygen ions, as illustrated in Fig. 23, curve C. Together with the studies by Setlow, this suggested that the higher the LET of the radiations, the smaller the temperature dependence of the inactivation processes, at least up to room temperature.

Fig. 23

Shalek (87) has recently carried out a very careful study of the radiosenstivity of lysozyme, exposed in H_2-atmosphere to Co^{60} γ-rays and electrons. With the kind permission of Dr. Shalek these previous unpublished results are presented in Fig. 23 (curves A and B), together with the present heavy ion inactivation data. Curve A shows the results obtained with γ-rays and curve B with electrons. The Co^{60} data were obtained with dose rates from 3000 to 25000 r/min, whereas the electron data were obtained with pulsed radiation of average dose rate about $14.4\ 10^6$ r/min. The latter dose rate is quite similar to that used in the heavy ion bombardments, the results of which are shown in curve C. While the radiosensitivity of lysozyme showed very little temperature dependence for C-ions (curve C), an increase of the radiosensitivity by about a factor of 4 was found after exposure

to electrons and to γ-rays when the sample temperature rose from 77° K to room temperature. The present heavy ion data are based on a single experiment, and considerable errors may be involved. Nevertheless it illustrates clearly that the temperature dependence of the radiosensitivity is intimately connected with the LET of the radiations used, at least up to room temperature. In the case of lysozyme (and also of trypsin (19), for which data are not shown here), the radiosensitivity appears to increase smoothly with increasing temperatures, without any indication of plateaus, as in the case of catalase, referred to above. A repeat of the latter experiment would be desirable in order to develop more definite ideas about the mechanisms involved. The indication that the radiosensitivity of lysozyme depends only little on the sample temperature below 0° C, when exposed to densely ionizing radiation, could partly imply that the temperature along the track of the heavy ion becomes sufficiently high for inactivation, regardless the sample temperature. For sparsely ionizing radiations the local energy concentration is lower and the actual temperature of the sample may become decisive for inactivation. In order to quantisize such mechanism, a detailed study of the radiosensitivity as a function of the sample temperature during exposure to radiations of different LET will be necessary. Such a study, as mentioned earlier, might also throw more light on the reasons for the rather large inactivation cross sections observed for enzymes exposed to very densely ionizing radiations.

3. Oxygen Effect.

As first shown by Alexander (2), dry preparations of enzymes do exhibit an increased radiosensitivity when exposed under appropriate conditions in dry oxygen atmosphere to radiations of low LET, as compared to that found in dry nitrogen atmosphere. This effect has been studied further by some authors (19, 21, 51, 86, 87). The oxygen effect is strongly dependent upon the temperature of the samples during irradiation and naturally enough upon the dose rate. The importance of these factors has also been studied by Shalek (87) in the case of lysozyme. Table XIII shows some of his figures.

Table XII

The oxygen effect in the dry state appears to depend on a variety of factors. Preliminary investigations with X-rays for instance, indicated that samples dried from solutions containing certain admixtures may show various degrees of oxygen sensitization. This is also apparent from the work of Butler and Robins (21) on trypsin. When slow heavy ions are used, no oxygen effect is found. With high energy heavy ions a small effect may appear, caused by the presence of δ-rays of sufficient energy to travel out of the heavy ion track core.

4. Effects of pH.

It was found by Appleyard (4) that the radiation inactivation volume of hemoglobin was a function of the pH of the medium in which the samples were dissolved after irradiation. A pH of 5 resulted in an inactivation volume 4 times larger than that found if it were dissolved at pH 7.

We have found that both lysozyme and trypsin, when pretrated in phosphate buffers of various pH and then subjected to densely ionizing radiations, showed variations in radiation sensitivity. With constant pH the radiosensitivity was found to be dependent also on the molarity of the phosphate buffer. Wilson (107) has reported on the influence of the pH of the solutions from which DNase has been dried.

It seems to the present author very important to consider enzymes which have been exposed to ionizing radiations not merely as active or inactive, which often is done in simple "target" analysis, but also to consider partially damaged enzyme molecules. Very interesting work with this approach has been reported by Augenstine (5) on X-ray and UV studies of trypsin in solutions. In the present study it was found that the radiosensitivity of dried trypsin exposed to 123 Mev Ne-ions at room temperature was the same, whether tested for its protease activity, employing hydrolysis of casein or its esterase activity, employing hydrolysis of N-benzoyl-L-arginine ethyl ester. However, if the protease activity was tested employing hydrolysis of hemoglobin (with 5.5 M urea), the radiosensitivity was about 1.7 times higher. This higher sensitivity may, as first suggested by Augenstine (5), be ascribed to an ability of urea to render partially damaged enzyme molecules inactive. The conclusion to be drawn is thus that the absorption of energy within an enzyme molecule in the dry state may damage the molecule, and whether or not it is counted as an inactive or active enzyme is dependent upon successive treatment.

The present discussion of the radiosensitivity of different enzymes exposed to ionizing radiations of varying LET's have

shown that the radiosensitivity depends on several factors including LET, admixtures of foreign substances, pH of the medium from which the samples are prepared and the buffer in which irradiated samples are resuspended, assay method, temperature during exposure and the presence of oxygen during exposure. The data support the idea that under appropriate conditions, migration of energy takes place between adjacent molecules depending upon properties of the enzyme and the surrounding molecules.

It is felt that the question of partially damaged molecules which subsequently may be completed inactivated by relatively small amounts of energy, warrants more thorough consideration. This was highlighted by the temperature dependence of the inactivation processes and by the dependence of the radiosensitivity upon the assay methods used as well as other post irradiation treatments (75). The stress experienced by enzymes during drying to obtain thin films on bombardment disks is of particular importance in this respect, and accounts for a substantial part of the variability of the radiosensitivity generally found in radiation inactivation of dried enzymes.

The presented track segment analysis of the radiosensitivity of dried, crystalline enzymes when account was taken of the entire LET-energy spectral distributions of the various radiations, indicated that a superabundancy of ionizations are formed if single ionizations are separated by shorter distances than about 10 Å/ρ.

V. SUMMARY

It has been known for many years that the spatial distribution of energy transfers, measured as LET, is among the many factors which contribute to the efficiency by which ionizing radiations affect biological materials. The main purpose of the present work, performed with the Berkeley Heavy Ion Linear Accelerator (HILAC) has been to provide experimental data under well defined conditions on the radiosensitivity of a variety of different biological systems over a much wider LET range than hitherto used in radiobiological investigations. The emphasis has been placed on induction of effects which depend exponentially upon the dose, without dose rate effects when induced under anoxic conditions.

Attempts to analyze the experimentally determined efficiencies by which the various effects are induced as a function of LET have also been made, based on two hypothetical mechanisms, originally proposed by Howard-Flanders. According to this hypothesis, the oxygen-independent component of the radiation injury is assumed to be the result of n or more ionizations, whereas the oxygen-dependent component of the injury is assumed to be the result of less than n ionizations in the track segment.

Quantitative expressions of the two mechanisms as a function of the mean number of ionizations in the track segment have been worked out. Furthermore, the use of these functions has been discussed in combination with the calculated complex LET versus energy distributions resulting from different types of heavy ions penetrating thin samples.

The LET dependency of the following effects has been subjected to investigation in the present paper:

1) Inhibition of the plaque-forming ability of T-1 bacteriophage exposed in dry state and in nutrient broth suspension.

2) Inhibition of the colony-forming ability of Shigella sonnei exposed under anoxia and in the presence of oxygen.

3) Inhibition of the colony-forming ability of haploid yeast cells, exposed both under anoxia and in the presence of oxygen, and the radioprotection provided by glycerol treatment.

4) Induction of dominant lethals in haploid yeast cells exposed under aerobic condition.

5) Inactivation of dried enzymes under a variety of experimental conditions.

The main results of the present investigation may be summarized as follows:

Two alternative relationships between relative biological efficiency (RBE) and LET were found:

1) The RBE decreases with increasing LET over the entire LET-range studied.

This was found to be the case for inhibition of the colony-forming ability of bacteria exposed in O_2-atmosphere, for inactivation of enzymes exposed in vacuum, and for inhibition of the plaque-forming ability of T-1 bacteriophage exposed both in vacuum and in nutrient broth suspension. In this latter case the presence of nutrient broth seems to increase the distance over which energy transfer via indirect action takes place by some 35 Å.

2) The RBE increases with increasing LET and then decreases when the LET exceeds a value characteristic for the effect studied.

This relationship was found for inhibition of the colony-forming ability of haploid yeast cells exposed both in N_2- and in C_2-atmospheres, for the inhibition of the colony-forming ability of bacteria exposed in N_2-atmosphere, and for induction of dominant lethals in haploid yeast exposed aerobically.

All effects studied in the present paper show a declining RBE with increasing LET when the LET exceeds1000 Mev.$gm.^{-1}$ $cm.^2$.

Glycerol treatment of haploid yeast cells provides a radio-protection which, under anoxia, is essentially independent of LET.

Biological systems exposed to fast, heavy ions usually show an oxygen effect, which is due to the delta rays produced by the heavy particle.

The radiosensitivity of dried enzymes is found to depend on a variety of factors. Thus, the efficiency of heavy ions to inactivate dried enzymes kept at various constant temperatures during the exposure differs markedly from that of sparsely ionising radiations.

The high efficiency for inactivation of dried enzymes by radiations of high LET, combined with the protective and sensitising effects provided by admixtures of certain foreign molecules, supports the idea of inter- and intra-molecular energy transfer processes.

Footnote:

The present track segment analysis differs somewhat from that of a previous treatment of some of these data (20), inasmuch as in the present work detailed account is taken of the LET-energy spectral distributions, and LET-values of slow electrons are calculated from the experimental measurements of Davis (31). Although there are reasons to believe that the amount of energy required to form an ion pair in a typical biological material is lower than that of, say N_2 gas, in lack of a better value 34.8 ev (12) was used in the present calculations.

TABLE I

Ranges of some heavy ions in Aluminium.

Particle	Measured range in Al. mg/cm^2	Reported energy (45) Mev/amu
Ne^{4}	100	10.4 ± 0.2
Ne^{11}	82	"
C^{12}	62.6	"
O^{16}	49.4	"
Ne^{20}	42.4	"
A^{40}	34	"

TABLE II

LET and Range in Tissue of some Heavy Ions of Energy 10 Mev/amu.

Particle	Calculated range in tissue, mg/cm^2	Calculated LET in tissue, $Mev\ gm^{-1}cm^2$
H^1	123	45
He^4	123	180
B^{11}	57	1145
C^{12}	44	1620
O^{16}	34	2900
Ne^{20}	29	4500
A^{40}	24	11000 [a]

a Not completely stripped.

TABLE III

Delta Ray Spectra of Heavy Ions of Different Energy (β = 100 ev).

Delta ray energy range (Mev)	IET Mev $gm^{-1}cm^2$	Local energy dissipation, $C_\beta \Delta T$. 10^{10} ev $gm^{-1}rad^{-1}$			
		10 Mev/amu	6.16 Mev/amu	4.2 Mev/amu	3.3 Mev/amu
19.2 - 25.6	7.82	5			
12.8 - 19.2	10.5	83	1		
9.6 - 12.8	13.9	103	43		
6.4 - 9.6	18.6	195	140	54	8
4.8 - 6.4	24.6	165	142	108	68
3.2 - 4.8	33.0	267	252	223	189
2.4 - 3.2	46.8	209	206	197	184
1.6 - 2.4	70.0	319	323	320	312
1.2 - 1.6	110	247	255	258	258
0.8 - 1.2	166	370	386	389	390
0.6 - 0.8	253	286	300	310	318
0.4 - 0.6	366	449	471	490	502
0.3 - 0.4	504	350	368	384	394
0.2 - 0.3	686	549	573	599	616
0.15 - 0.2	810	405	426	447	460
0.1 - 0.15	902	624	659	688	709
0 - 0.1	930	1612	1698	1775	1829
$\sum C_\beta \Delta T$		6243	6243	6243	6243

Mean, delta ray energy (Mev)	22.4	13.5	9.3	7.3
~~Reciprocal of [illegible] ($gm^{-1}cm^2$)~~	~~11.9~~	~~18.1~~	~~16.4~~	~~20.3~~
"Energy average" IET (Mev $gm^{-1}cm^2$)	476.4	549.5	574.0	583.1
Fraction of total energy dissipated by heavy ions as delta rays	0.445	0.452	0.459	0.457

TABLE IV.

P(n) as a Function of m, the Average Number of Ionizations in the Track Segment "t".

m	n=1	n=2	n=3	n=4	n=5	n=6	n=7	n=8	n=9	n=10
0	0.5025	0.2513	0.1256	0.0754	0.0352	0.0101	0.0000	0.0000	0.0000	0.0000
0.0199	0.5000	0.2512	0.1262	0.0759	0.0357	0.0105	0.0003	0.0001	0.0001	0.0000
0.199	0.4782	0.2511	0.1318	0.0809	0.0400	0.0142	0.0027	0.0012	0.0005	0.0002
0.398	0.4585	0.2497	0.1367	0.0852	0.0452	0.0188	0.0063	0.0034	0.0018	0.0010
0.995	0.3955	0.2431	0.1478	0.0988	0.0576	0.0300	0.0142	0.0077	0.0042	0.0024
1.393	0.3613	0.2366	0.1524	0.1031	0.0649	0.0359	0.0199	0.0114	0.0065	0.0037
1.99	0.3176	0.2252	0.1559	0.1104	0.0744	0.0469	0.0281	0.0171	0.0104	0.0062
2.985	0.2602	0.2042	0.1551	0.1176	0.0862	0.0605	0.0408	0.0272	0.0179	0.0117
3.980	0.2173	0.1897	0.1492	0.1197	0.0934	0.0704	0.0514	0.0367	0.0259	0.0180
4.970	0.1891	0.1466	0.1310	0.1144	0.0975	0.0811	0.0656	0.0520	0.0405	0.0311
7.960	0.1233	0.1107	0.1118	0.1032	0.0934	0.0821	0.0717	0.0610	0.0509	0.0419
9.950	0.0998	0.0981	0.0952	0.0910	0.0856	0.0791	0.0720	0.0643	0.0565	0.0491
13.930	0.0717	0.0715	0.0710	0.0700	0.0686	0.0667	0.0642	0.0610	0.0574	0.0534
19.900	0.0502	0.0502	0.0502	0.0501	0.0500	0.0497	0.0493	0.0487	0.0479	0.0469
29.850	0.0335	0.0335	0.0335	0.0335	0.0335	0.0335	0.0335	0.0335	0.0335	0.0334
39.800	0.0251	0.0251	0.0251	0.0251	0.0251	0.0251	0.0251	0.0251	0.0251	0.0251
59.700	0.0167	0.0167	0.0167	0.0167	0.0167	0.0167	0.0167	0.0167	0.0167	0.0167
79.600	0.0126	0.0126	0.0126	0.0126	0.0126	0.0126	0.0126	0.0126	0.0126	0.0126
99.500	0.0101	0.0101	0.0101	0.0101	0.0101	0.0101	0.0101	0.0101	0.0101	0.0101
199.0	0.0050	0.0050	0.0050	0.0050	0.0050	0.0050	0.0050	0.0050	0.0050	0.0050
995.0	0.0010	0.0010	0.0010	0.0010	0.0010	0.0010	0.0010	0.0010	0.0010	0.0010
1990.0	0.0005	0.0005	0.0005	0.0005	0.0005	0.0005	0.0005	0.0005	0.0005	0.0005

TABLE 7.

P(s) as a Function of m, the Average Number of Ionizations in the Track Segment "t".

m	s=1	s=2	s=3	s=4	s=5	s=6	s=7	s=8	s=9	s=10
0	0.2512	0.1257	0.0502	0.0402	0.0251	0.0101	0.0000	0.0000	0.0000	
0.0199	0.2483	0.1250	0.0503	0.0402	0.0252	0.0102	0.0002	0.0000	0.0000	
0.199	0.2271	0.1193	0.0509	0.0409	0.0258	0.0115	0.0015	0.0007	0.0003	
0.398	0.2058	0.1130	0.0515	0.0400	0.0264	0.0125	0.0029	0.0016	0.0008	
0.995	0.1524	0.0953	0.0510	0.0392	0.0276	0.0158	0.0065	0.0035	0.0018	
1.393	0.1247	0.0842	0.0493	0.0382	0.0290	0.0160	0.0085	0.0049	0.0028	
1.99	0.0924	0.0693	0.0455	0.0360	0.0275	0.0168	0.0110	0.0067	0.0042	
2.985	0.0560	0.0491	0.0375	0.0314	0.0257	0.0197	0.0135	0.0093	0.0062	
3.980	0.0336	0.0345	0.0295	0.0263	0.0230	0.0190	0.0147	0.0103	0.0079	
5.970	0.0125	0.0156	0.0166	0.0169	0.0164	0.0155	0.0136	0.0115	0.0094	
7.96	0.0046	0.0069	0.0086	0.0098	0.0119	0.0104	0.0107	0.0101	0.0090	
9.95	0.0017	0.0029	0.0042	0.0054	0.0065	0.0071	0.0077	0.0078	0.0074	
13.93	0.0002	0.0005	0.0010	0.0014	0.0019	0.0025	0.0032	0.0036	0.0040	
19.90	0.0000	0.0000	0.0001	0.0001	0.0003	0.0004	0.0006	0.0008	0.0010	
29.85	0	0	0	0	0	0	0	0.0002	0.0001	
39.80	0	0	0	0	0	0	0	0	0	
59.70	0	0	0	0	0	0	0	0	0	
79.60	0	0	0	0	0	0	0	0	0	
99.50	0	0	0	0	0	0	0	0	0	
199.0	0	0	0	0	0	0	0	0	0	
995.0	0	0	0	0	0	0	0	0	0	
1990.0	0	0	0	0	0	0	0	0	0	

TABLE VI.

Parameters Used in the Track Segment Analysis of T-1 Data.

Exposure conditions	Number of ionizations per track length (t) (sensitivity function)	Track length (t)	Sensitivity parameter (k) rad^{-1}
Dry state	1 or more (P(n=1))	8.7 Å/ρ	2.49 10^{-6}
Wet state	1 or more (P(n=1))	43.3 Å/ρ	20.9 10^{-6}

ρ is the numerical value of the density of the biological material.

TABLE VII.

Effect of Particle Velocity and LET on the Oxygen Effect.

Radiation	Track core LET Mev $gm^{-1}cm^2$	Energy/nucleon Mev/amu	Sensitivity in O_2 / Sensitivity in N_2
He-ions	89	9.8	1.6
He-ions	190	3.8	1.4
He-ions	337	1.9	1.06
B -ions	670	8.9	1.4
C -ions	990	8.4	1.4

TABLE VIII.

Parameters Used in the Track Segment Analysis of Shigella sonnei

Gas present during the exposure	Number of ionizations per track length (t) (Sensitivity function)	Track segment (t)	Sensitivity parameter (k) rad^{-1}	(ρ)
N_2	6 or more (P(n=6))	91 Å/ρ	$19.5\ 10^{-4}$	-
O_2	P(u=5)	91 Å/ρ	$19.5\ 10^{-4}$	0.63

ρ is the numerical value of the density of the sample material.

TABLE IX

Parameters Used in the Track Segment Analysis of Haploid Yeast.

Cells exposed in	Gas present during the exposure	Number of ionizations per track length (t) (Sensitivity function)	Track length (t)	Sensitivity parameter (k) rad^{-1}	ω
6 M glycerol	N_2	10 or more (P(n=10))	69 $\AA/\rho$	$14.04\ 10^{-4}$	-
6 M glycerol	Air	10 or more (P(n=10))	69 $\AA/\rho$	$14.04\ 10^{-4}$	-
PO_4 buffer	N_2	10 or more (P(n=10))	69 $\AA/\rho$	$26.17\ 10^{-4}$	-
PO_4 buffer	Air	P(n=9)	69 $\AA/\rho$	$26.17\ 10^{-4}$	0.20

ρ is the numerical value of the density of the sample material.

TABLE X.

Parameters Used in the Track Segment Analysis of Dominant Lethals.

Cells exposed in	Gas present during the exposure	Number of ionizations per track length (t) (Sensitivity function)	Track length (t)	Relative sensitivity parameter $(1/D_{37})rad^{-1}$	ω
H_2O	N_2	10 or more (P(n=10))	40 Å/ρ	$34.4\ 10^{-5}$	-
H_2O	Air	P(u=9)	40 Å/ρ	$34.4\ 10^{-5}$	0.20

ρ is the numerical value of the density of the sample material.

TABLE XI

Parameters Used in the Track Segment Analysis of the Enzyme Data.

Enzyme	Exposure conditions	Number of ionizations per track length (t) (Sensitivity function)	Track length (t)	Sensitivity parameter (k) rad^{-1}
Lysozyme	vacuum	1 or more (P(n=1)	9.9 Å/ρ	$3.62\ 10^{-8}$
Trypsin	vacuum	1 or more (P(n=1)	9.9 Å/ρ	$4.96\ 10^{-8}$
DNase	vacuum	1 or more (P(n=1)	11.5 Å/ρ	$7.45\ 10^{-8}$

ρ is the numerical value of the density of the sample material.

TABLE XII

Reported and Deduced Molecular Weights of the Enzymes Studied.

Enzyme	Reported molecular weight	Molecular weights from present analysis
Lysozyme	14700 ±250 (42)	37000
Trypsin	23000 (56)	50000
DNase	63000 (55)	80000

TABLE XIII

The Oxygen Effect of Insecmis as a Function of Dose Rate and Sample Temperature (87).

Dose rate range r/min.	Sensitivity in O_2 / Sensitivity in N_2				
	77° K	195° K	273° K	295° K	299° K
3000 - 25000		1.12	1.65	1.83	
$14.4\ 10^6$ (average)	1.06				1.22

FIG. 1. The experimental setup used for heavy ion exposure.

FIG. 2. (a) The track density of carbon ions across the diameter of the beam cross section, showing a somewhat skew distribution. (b) Range distribution (energy distribution) of carbon ions at the sample position.

FIG. 3. Bombardment chamber used for exposure of samples kept at various temperatures and in different gas atmospheres during the exposure.

FIG. 4. Design of the ionization chamber and the bombardment compartment.

FIG. 5. Typical voltage saturation curves of the chamber diagrammed in Fig. 4, for different dose rates of carbon ions.

FIG. 6. External Faraday current relative to the monitor current as a function of the thickness of Al absorbers, for carbon, oxygen, and neon ions.

FIG. 7. Bragg curves in tissue of Ne^{20}, O^{16}, C^{12}, and B^{11} of initial energy 10.4 $\pm$ 0.2 Mev/amu. The area under each curve is shown.

FIG. 8. LET-energy distributions of different heavy ions of energy 9.3 Mev/amu. The hatched area is the LET-energy spectrum of the delta electrons, which should be included in the LET-energy distribution of each of the heavy ions shown. (See text).

FIG. 9. LET-energy distributions of different heavy ions of energy 10 Mev/amu. The hatched area is the LET-energy spectrum of the delta electrons, which should be included in the LET-energy distribution of each of the heavy ions shown. (See text).

FIG. 10. Three hypotetical probability functions.

FIG. 11. The probability of n or more ionisations in the track segment "t", divided by the average number of ionisations in this segment, P(n), as a function of the average number of ionisations on "t" (m).

FIG. 12. The probability of just s ionizations (i.e. s and s only) in the track segment "t" divided by the average number of ionisations in this segment, P(s), as a function of the average number of ionizations in "t" (m).

FIG. 13. The radiosensitivity of T-1 bacteriophage exposed aerobically in nutrient broth, and in dry state and high vacuum, as a function of the LET of the radiations. The dotted line on the dry state curve represents the average value of a great many experiments, within which LET-range the sensitivity was found constant (38). The solid curves are calculated according to track segment hypothesis. (See text).

FIG. 14. The radiosensitivity of Shigella sonnei exposed in O_2 atmosphere and in N_2 atmosphere respectively, as a function of the LET of the radiations. The curves are calculated according to track segment hypothesis. (See text).

FIG. 15. Illustration of the dependence of the oxygen enhancement ratio (open circles) and the maximum energy transferred to delta electrons (filled squares), as a function of the energy per nucleon of He-ions.

FIG. 16. The radiosensitivity as a function of LET of haploid Saccharomyces cerevisiae, exposed under different conditions, tested by the inhibition of colony formation. The curves are calculated according to track segment hypothesis. (See text).

FIG. 17. The per cent surviving zygotes as a function of the dose of different radiations.

FIG. 18. The radiosensitivity of haploid Saccharomyces cerevisiae exposed in oxygen atmosphere, as a function of the LET, tested by the inhibition of zygote formation. The solid curve is calculated according to the track segment hypothesis. (See text).

FIG. 19. The radiosensitivity of lysozyme, trypsin, and Diase as a function of the LET of the radiations. The solid curves are calculated according to the track segment hypothesis. (See text).

FIG. 20. Inactivation cross section of lysozyme, trypsin, and DNase as a function of the total stopping power, (dE/dx) of the radiations used.

FIG. 21. Attempts to fit theoretical curves (dotted) based on simple target theoretical considerations of different "target sizes" to the directly observed inactivation data (solid curve). The calculated effects of δ-rays are included in the theoretical curves.

FIG. 22. Inactivation cross section of trypsin mixed with dextran, ribose, cysteine, and pinacyanole as a function of R, the ratio of foreign molecules per trypsin molecule. Radiation: 115 Mev carbon ions.

FIG. 23. Relative radiosensitivity of lysozyme exposed at various temperatures to different radiations. Curve A: Co^{60} γ-rays, "low" dose rate. Curve B: electrons, "high" dose rate. Curve C: O-ions, "high" dose rate. Curves A and B are due to Shalek (37). (See text).

REFERENCES

1. Alexander, P., and Charlesby, A., Nature 173, 578 (1954).
2. Alexander, P., Radiation Research 6, 653 (1957).
3. Alvarez, L. W., Phys. Rev. 58, 192 (1940).
4. Appleyard, R. K., Arch. Biochem. Biophys. 35, 121 (1952).
5. Augenstine, L. Science 128, 718 (1959).
6. Beekman, W. J., Physica 15, 327 (1949).
7. Beringer, R., Gluckstern, R. L., Malkin, M. S., Hubbard, E. L., Smith, L., and Van Atta, C. M., University of California Radiation Laboratory Report. UCRL-2796 (1954).
8. Bethe, H., Ann. Physik 5, 325 (1930).
9. Bethe, H., Z. Phys. 76, 293 (1932).
10. Bethe, H., and Ashkin, J., in "Experimental Nuclear Physics", (E. Segre, ed.) Vol. 1, p. 166, Wiley, New York, 1953.
11. Birge, A. C., and Tobias, C. R., Arch. Biochem. Biophys. 52, 388 (1954).
12. Birge, A. C., Anger, H. O., and Tobias, C. A., in "Radiation Dosimetry", (G. J. Hine and G. L. Brownell, eds.), p. 623. Academic Press, New York, 1956.
13. Birge, A. C., and Sayeg, J. A., Radiation Research 10, 433, (1959).
14. Blau, M., and Altenburger, K., Z. Phys. 12, 315 (1923).
15. Boag, J. W., Report. National Bureau of Standards, Washington, D. C. NBS-2946. (1953).
16. Boag, J. W., in "Radiation Dosimetry" (G. J. Hine and G. L. Brownell, eds.), p. 153. Academic Press, New York, 1956.

17. Braams, R., Hutchinson, F., and Ray, D., Nature 182, 1506 (1958).

18. Braams, R., Radiation Research 12, 113 (1960).

19. Brustad, T., Radiation Research, Suppl. 2, 65 (1960).

20. Brustad, T., Radiation Research 15, 139 (1961).

21. Butler, J. A. V., and Robins, A. B., Nature 186, 697 (1960).

22. Burch, P. R. J., Radiation Research 3, 361 (1955).

23. Burch, P. R. J., and Bird, P. M., in "Progress in Radiobiology" (J. S. Mitchell, B. E. Holmes, and C. L. Smith, eds.) p. 161. Oliver & Boyd, Edinburgh, Scotland, 1956.

24. Burch, P. J. R., Radiation Research 6, 289 (1957).

25. Burch, P. R. J., Brit. J. Radiol. 30, 524 (1957).

26. Buzzati-Traverso, A., and Cavalli, L.L., "Teoria dell'urto ed unith biologiche elementari". Longanesi, Milan, 1948.

27. Conger, A. D., Randolph, M. L., Sheppard, C. W., and Luippold, H. J., Radiation Research 9, 525 (1958).

28. Cormack, D. V., and Johnes, H. E., Brit. J. Radiol. 25, 369 (1952).

29. Curtis, H. J., Science 133, 312 (1961).

30. Dale, W. M., Meredith, W. J., and Tweedie, M. C. K., Nature 151, 280 (1943).

31. Davis, M., Phys. Rev. 94, 243 (1954).

32. Deering, R. A., Radiation Research 14,460 (1961). Abstract.

33. Dittrich, W., Z. Naturforschg. 15 b, 261 (1960).

34. Dolphin, G. W., and Hutchinson, F., Radiation Research 13, 403 (1960).

35. Fano, U., in "Radiation Biology" (A. Hollaender, ed.) Vol. I, part I, p. 1. McGraw-Hill, New York, 1954.

36. Fluke, D. J., and Pollard, E. C., Ann. N.Y. Acad. Sci. 59, 484 (1955).

37. Fluke, D. J., Brustad, T., and Birge, A. C., Radiation Research 13, 788 (1960).

38. Fluke, D.J. and Forro, F., Jr., Radiation Research 13, 305, (1960).

39. Forro, F., Jr., and Fluke, D.J., Radiation Research 3, 225, (1955). Abstract.

40. Freier, P., Loefgren, E. J., Ney, E. P., Oppenheimer, F., Bradt, H. L., and Peters, B., Phys. Rev. 74, 213 (1948).

41. Fricke, H., and Brownscombe, E. R., Phys. Rev. 44, 240 (1933).

42. Fromageot, C, and de Garilhe, M. P., Biochim. et Biophys. Acta 4, 509 (1950).

43. Giles, N., Proc. Natl. Acad. Sci., U.S. 26, 567 (1940).

44. Gray, L. H., Brit. J. Radiol. Suppl. 1, 7 (1947).

45. Heckman, H. H., Perkins, B. L., Simon, W. G., Smith, F. M., and Barkas, W. H., Phys. Rev. 117, 544 (1960).

46. Hewitt, H. B., and Read, J., Brit. J. Radiol. 23, 416 (1950).

47. Howard-Flanders, P., and Alpher, T., Radiation Research 7, 518 (1957).

48. Howard-Flanders, P., in "Advances in Biological and Medical Physics" (C.A. Tobias, and J. H. Lawrence, eds.) Vol. VI, p. 553. Academic Press, New York, 1958.

49. Howard-Flanders, P., Nature 186, 485 (1960).

50. Hutchinson, F., Radiation Research 7, 473 (1957).

51. Hutchinson, F., Radiation Research, Suppl. 2, 49 (1960).

52. Hutchinson, F., and Easter, S. S., Jr., Science 132, 1311 (1960).

53. Hutchinson, F., and Norcross, C., Radiation Research 12, 13 (1960).

54. Jesse, W. P., Phys. Rev. 122, 1195 (1961).

55. Kunitz, M., J. gen. Physiol. 33, 349 (1950).

56. Laskowski, M., in "Methodes in Enzymology" (S. P. Colowick and N. O. Kaplan, eds.) Vol. 2, p. 26. Academic Press, New York, 1955.

57. Lea, D. E., Haines, R. B., and Bretscher, E., J. Hyg. 41, 1 (1941).

58. Lea, D. E., "Actions of Radiations on Living Cells", Cambridge University Press, London, 1946.

59. McNulty, W. P., Jr., and Hutchinson, F., Arch. Biochem. Biophys. 50, 92 (1954).

60. Manney, T. R., Brustad, T., Barr, J., and Tobias, C. A., Radiation Research 11, 453 (1959). Abstract.

61. Manney, T. R., Brustad, T., Barr, J., and Tobias, C. A., Radiation Research 12, 455 (1960). Abstract.

62. Marcovich, H., Radiation Research 9, 149 (1958). Abstract.

63. Marcovich, H., Thesis (1959).

64. Mortimer, R. K., Radiation Research 2, 361 (1955).

65. Mortimer, R. K., and Brustad, T., Radiation Research 12, 458 (1960). Abstract.

66. Neurnberger, C. E., J. Chem. Phys. 4, 697 (1936).

67. Norman, A., and Cinoza, W., Radiation Research 9, 77 (1958).

68. Northcliffe, L. C., Phys. Rev. 120, 1744 (1960).

69. Owen, M. E., and Mortimer, R. K., Nature 177, 625 (1956).

70. Platzman, R., and Franck, J., in "Symposium on Information Theory in Biology" (H. P. Yockey, R. L. Platzman, and H. Quastler, eds.) p. 262. Pergamon Press, New York, 1958.

71. Pollard, E. C., Powell, W. F., and Reaume, S. H., Proc. Natl. Acad. Sci., U.S. 38, 173 (1952).

72. Pollard, E. C., Guild, W. R., Hutchinson, F., and Setlow, R.B., in "Progress in Biophysics" (J. A. V. Butler and J.T. Randall, eds.) Vol. 5, p. 72. Pergamon Press, London, 1955.

73. Powers, E. L., Ehret, C.F., and Smaller, B., "Free Radicals in Biological Systems", p. 351. Academic Press, New York, 1960.

74. Powers, E. L., and Kaleta, B. F., Science 132, 959 (1960).

75. Powers, E. L., Webb, R.B., and Ehret, C. F., Radiation Research Suppl. 2, 94 (1960).

76. Powers, E. L., Smaller, B., Tobias, C. A., Lyman, J., and Brustad, T., "Abstracts of Contributed Papers", Int. Biophys. Congress, Stockholm, 1961, p. 96.

77. Rosenberg, A. M., Thesis, Univ. of Pennsylvania, Philadelphia (1958).

78. Sayeg, J. A., Birge, A.C., Beam, C. A., and Tobias, C. A., Radiation Research 10, 449 (1959).

79. Schaefer, H. J., U.S. Naval School of Aviation Medicine, Research Project MR005. 13-1002, Subtask 1, Report No. 16 (1959).

80. Schaefer, H. J., U.S. Naval School of Aviation Medicine, Research Project MR005. 13-1002, Subtask 1, Report No. 17 (1960).

81. Schaefer, H. J., Aerospace Med. 31, 807 (1960).

82. Schambra, P. E., Rauth, A. M., and Northcliffe, L. C., Phys. Rev. 120, 1758 (1960).

83. Schneider, D. O., and Cormack, D. V., Radiation Research 11, 418 (1959).

84. Schwert, G. W., and Takenaka, Y., Biochim. et Biophys. Acta 16, 570 (1955).

85. Setlow, R. B., Proc. Natl. Acad. Sci., U.S. 38, 166 (1952).

86. Shalek, R. J., "Twelfth Annual Symposium on Fundamental Cancer Research," University of Texas, Austin, Texas, 1958.

87. Shalek, R. J., Personal communication (1961).

88. Shugar, D., Biochim. et Biophys. Acta 8, 302 (1952).

89. Simons, D. G., in "Medical Physics" (O. Glasser, ed.) Vol. 3, p. 64. Year Book Publ., Chicago, 1960.

90. Sommermeyer, K., in "Strahlenbiologie, Strahlentherapie, Nuclearmedizin und Krebsforschung. Ergebnisse 1952-1958" (H. R. Schinz, H. Holthausen, H. Langendorff, B. Rajewsky, and G. Schubert, eds.) p. 1. Georg Thieme Verlag, Stuttgart, Germany, 1959.

91. Spencer, L. V., and Faro, U., Phys. Rev. 93, 1172 (1954).

92. Spencer, L. V., and Attix, F. H., Radiation Research 3, 239 (1955).

93. Spiers, F. W., in "Radiation Dosimetry" (G. J. Hine and G. L. Brownell, eds.) p. 1. Academic Press, New York, 1956.

94. Stapleton, G. E., Hollaender, A., and Martin, F. L., J. Cell. Comp. Physiol. 39, Suppl. 1, 87 (1952).

95. Stent, G. S., in "Advances in Virus Research" (K. M. Smith, and M. A. Lauffer, eds.) Vol. 5, p. 95. Academic Press, New York, 1958.

96. Sternheimer, R. M., Phys. Rev. 91, 256 (1953).

97. Timofeeff-Ressovsky, N. W., and Zimmer, K. G. "Das Treffer-prinzip in der Biologie. Biophysik," Band 1. S. Hirzel Verlag, Leipzig, 1947.

98. Tobias, C. A., and Segre, E., Phys. Rev. 70, 89 (1946).

99. Tobias, C. A., Weymouth, P. P., Wasserman, L. R. and Stapleton, G. E., Science 107, 115 (1948).

100. Tobias, C. A., in "Symposium on Radiobiology" (J. J. Nickson, ed.) p. 357. Wiley, New York, 1952.

101. Tobias, C. A., University of California Radiation Laboratory Report, UCRL-8115 (1958).

102. Van Allen, J. A., in "Physics and Medicine of the Atmosphere and Space" (O. O. Benson, Jr., and Strughold, H. eds.) Wiley, New York, 1960. (See also many other articles in the same book).

103. Van Atta, C. M., and Hubbard, E. L., University of California Radiation Laboratory Report, UCRL-3782 (1957).

104. Watson, J. D., J. Bacteriol. 63, 473 (1952).

105. Williams, R. C., and Fraser, D., J. Bacteriol. 66, 458 (1953).

106. Wilson, C. T. R., Proc. Roy. Soc. A104, 192 (1923).

107. Wilson, D. E., Int. J. Rad. Biol. 1, 360 (1959).

108. Wood, T. H., Proc. Soc. Exp. Biol. Med. 84, 446 (1953).

109. Wood, T. H., Ann. Rev. Nucl. Sci. 8, 343 (1958).

110. Wyckoff, R. W. G., J. Exp. Med. 52, 769 (1930).

111. Zelle, M. R., and Hollaender, A., in "Radiation Biology" (A. Hollaender, ed.) Vol. 2, p. 365. McGraw-Hill, New York, 1955.

112. Zimmer, K. G., "Studies on Quantitative Radiation Biology". Oliver & Boyd, Edinburgh, Scotland, 1961.

113. Zirkle, R. E., J. Cell. Comp. Physiol. 16, 221 (1940).

114. Zirkle, R. E., Marchbank, D. F., and Kuck, K. D., J. Cell. Comp. Physiol. 39, Suppl. 1, 75 (1952).

115. Zirkle, R. E., in "Symposium on Radiobiology" (J. J. Nickson, ed.) p. 333. Wiley, New York, 1952.

116. Zirkle, R. E., and Tobias, C. A., Arch. Biochem. Biophys. 47, 282 (1953).

117. Zirkle, R. E., in "Radiation Biology" (A. Hollaender, ed.) Vol. 1, part I, p. 315. McGraw-Hill, New York, 1954.

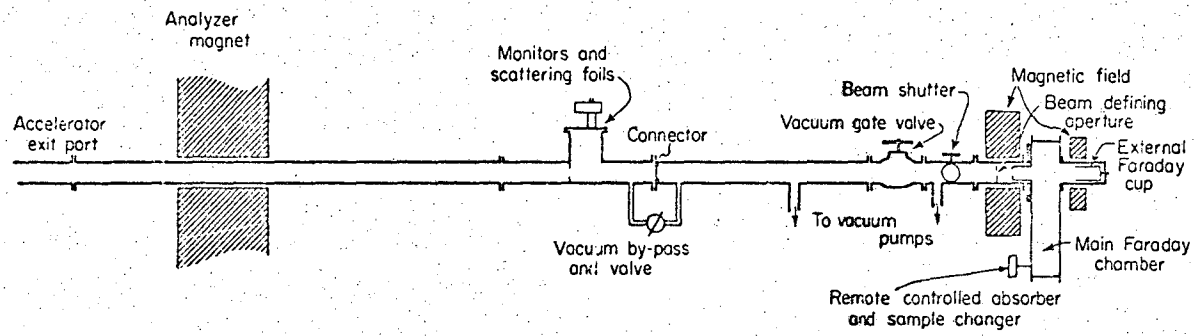
Analyzer magnet
Accelerator exit port
Monitors and scattering foils
Connector
Vacuum by-pass and valve
Beam shutter
Vacuum gate valve
To vacuum pumps
Magnetic field
Beam defining aperture
External Faraday cup
Main Faraday chamber
Remote controlled absorber and sample changer
ANALYZER SECTION
MONITOR SECTION
TARGET SECTION

Fig. 1

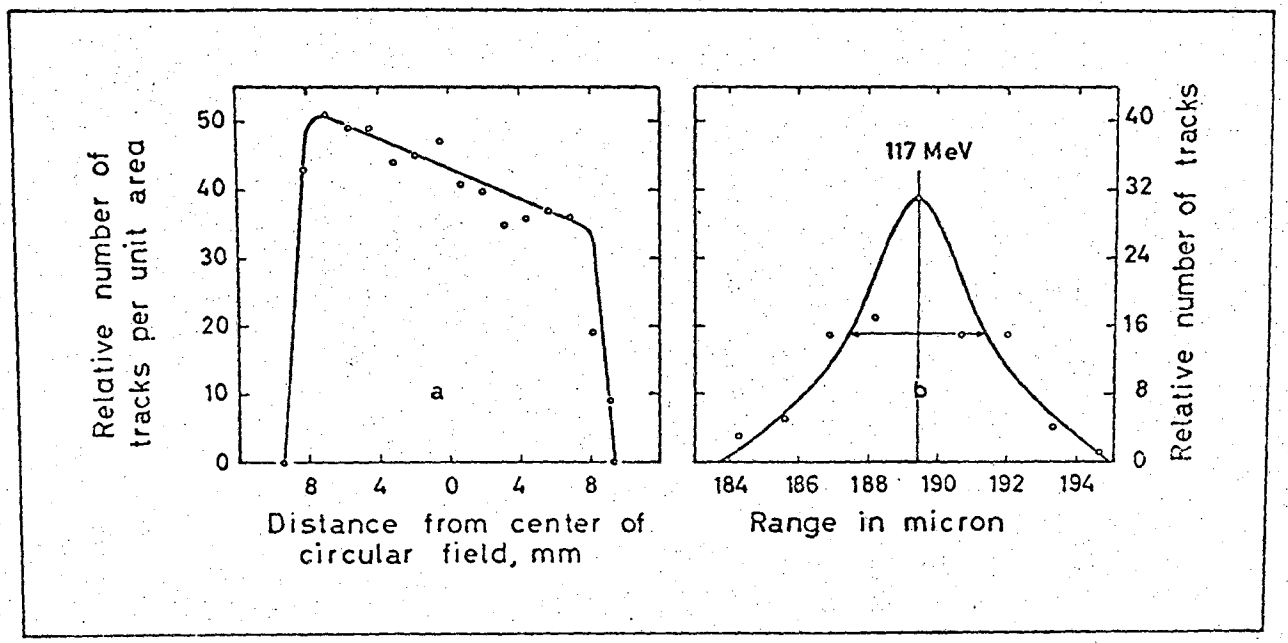
Relative number of tracks per unit area
50
40
30
20
10
0
8
4
0
4
8
a
Distance from center of circular field, mm
117 MeV
40
32
24
16
8
0
184
186
188
190
192
194
b
Range in micron
Relative number of tracks

Fig. 2

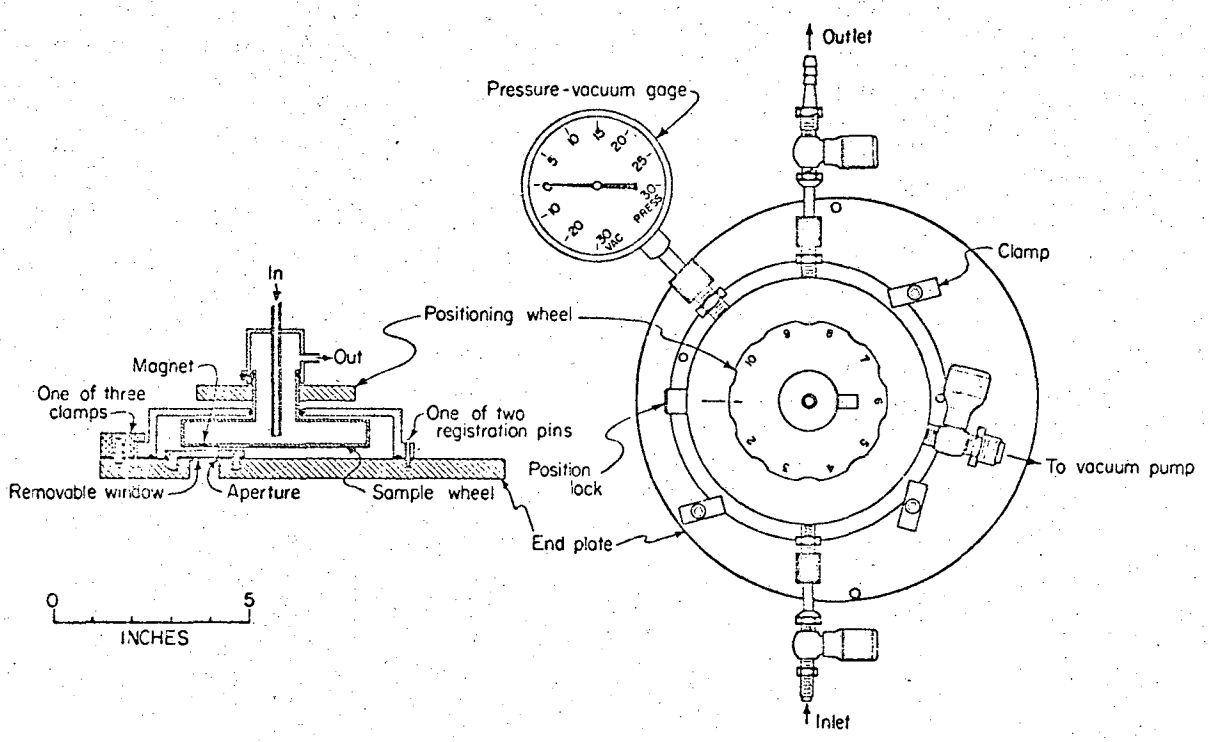
Outlet
Pressure-vacuum gage
Clamp
In
Positioning wheel
Out
Magnet
One of three clamps
One of two registration pins
Position lock
To vacuum pump
Removable window
Aperture
Sample wheel
End plate
0
5
INCHES
Inlet

Fig. 3

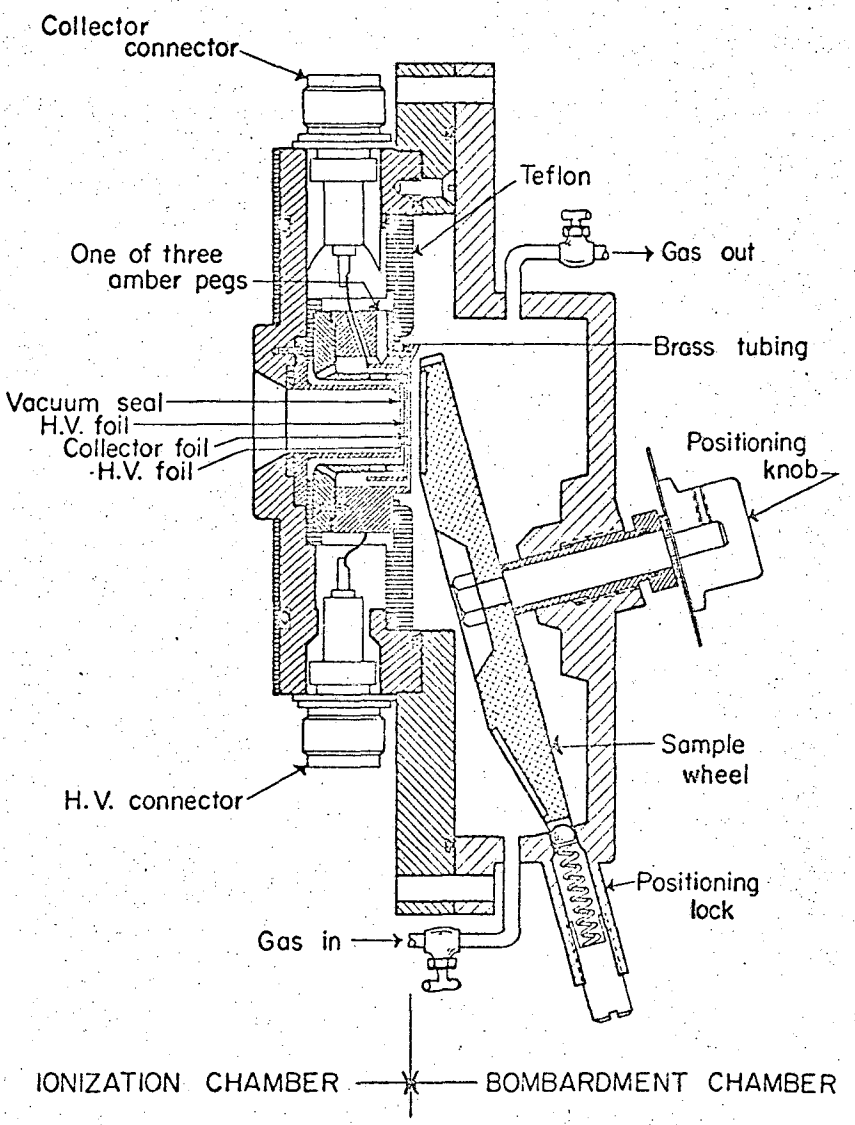
Collector connector
Teflon
One of three amber pegs
Gas out
Brass tubing
Vacuum seal
H.V. foil
Collector foil
H.V. foil
Positioning knob
Sample wheel
H.V. connector
Positioning lock
Gas in
IONIZATION CHAMBER
BOMBARDMENT CHAMBER

Fig. 4

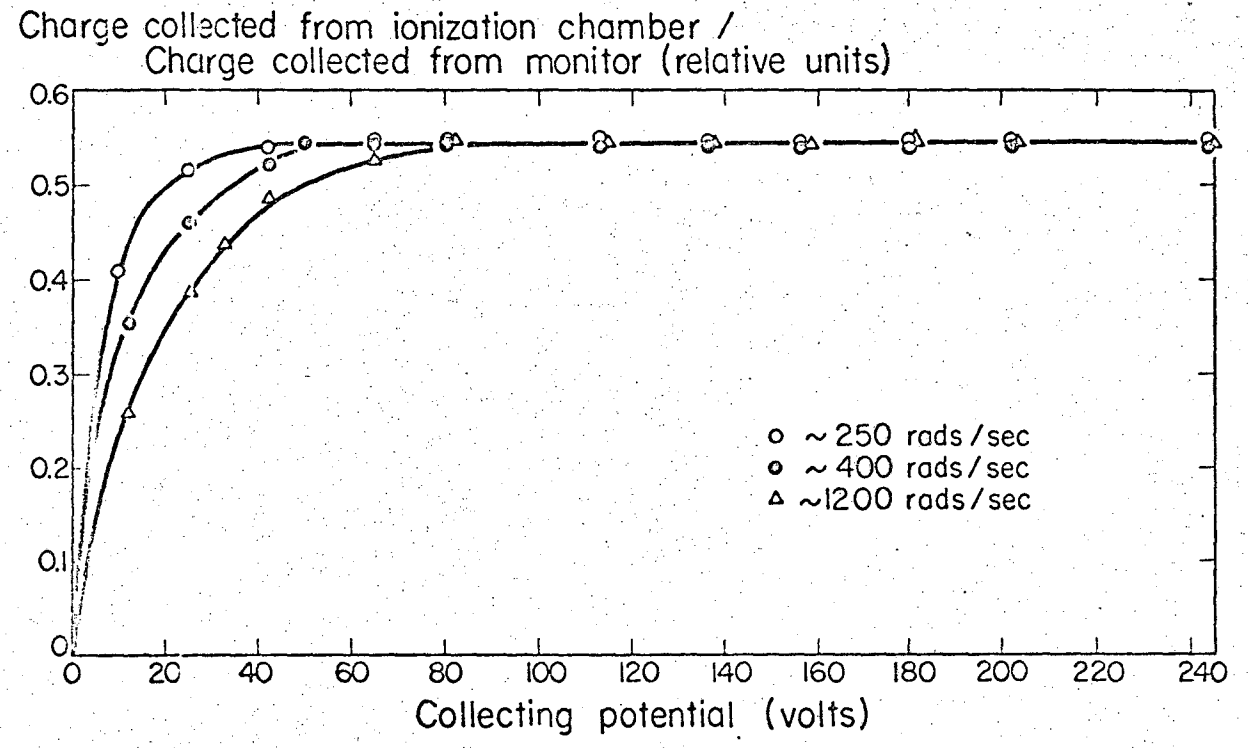
Charge collected from ionization chamber /
Charge collected from monitor (relative units)
0.6
0.5
0.4
0.3
0.2
0.1
0
0
20
40
60
80
100
120
140
160
180
200
220
240
Collecting potential (volts)
~250 rads/sec
~400 rads/sec
~1200 rads/sec

Fig. 5

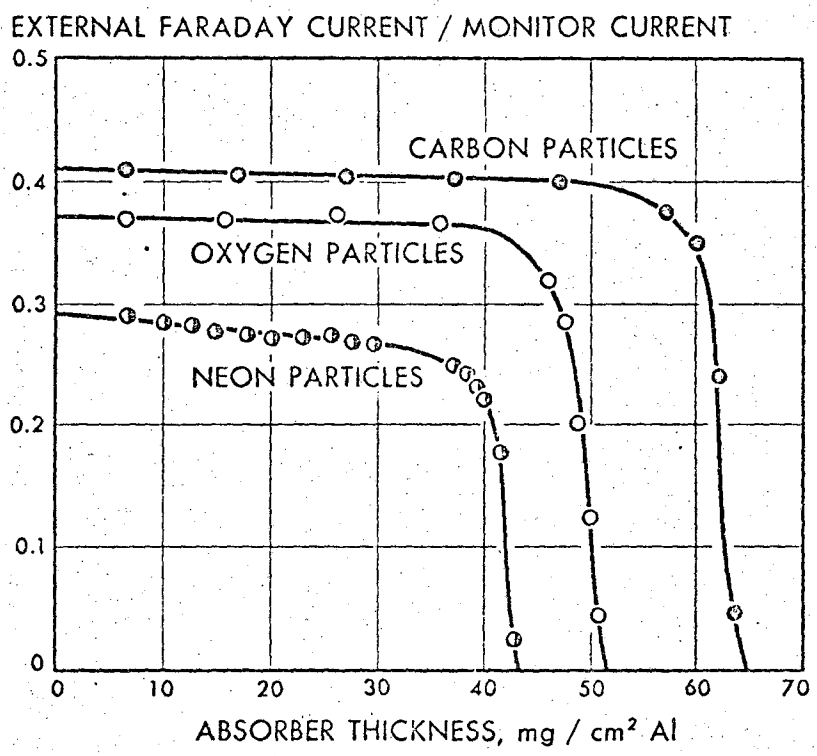
EXTERNAL FARADAY CURRENT / MONITOR CURRENT
0.5
0.4
0.3
0.2
0.1
0
CARBON PARTICLES
OXYGEN PARTICLES
NEON PARTICLES
0
10
20
30
40
50
60
70
ABSORBER THICKNESS, mg / cm² Al

Fig. 6

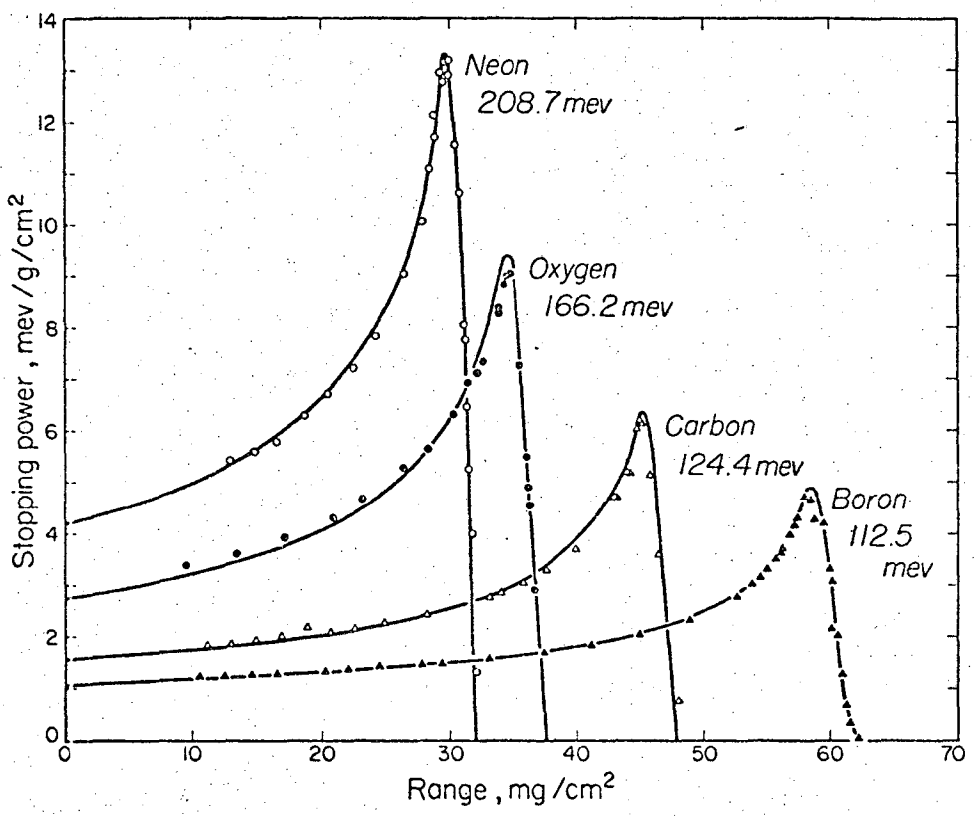
Neon
208.7 mev
Oxygen
166.2 mev
Carbon
124.4 mev
Boron
112.5
mev
Stopping power, mev/g/cm²
Range, mg/cm²
0
2
4
6
8
10
12
14
0
10
20
30
40
50
60
70

Fig. 7

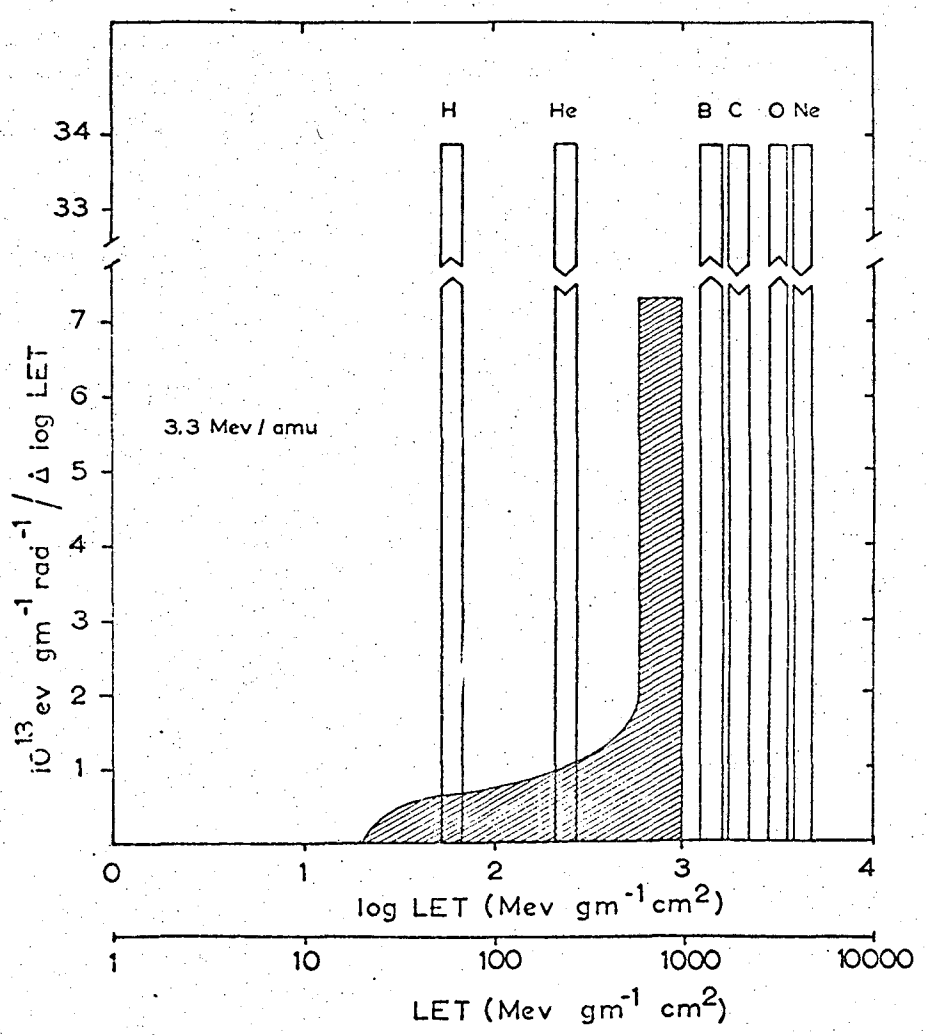
H
He
B C O Ne
34
33
7
6
5
4
3
2
1
3.3 Mev / amu
10^{13} ev gm^{-1} rad^{-1} / Δ log LET
0
1
2
3
4
log LET (Mev gm^{-1}cm^2)
1
10
100
1000
10000
LET (Mev gm^{-1} cm^2)

Fig. 8

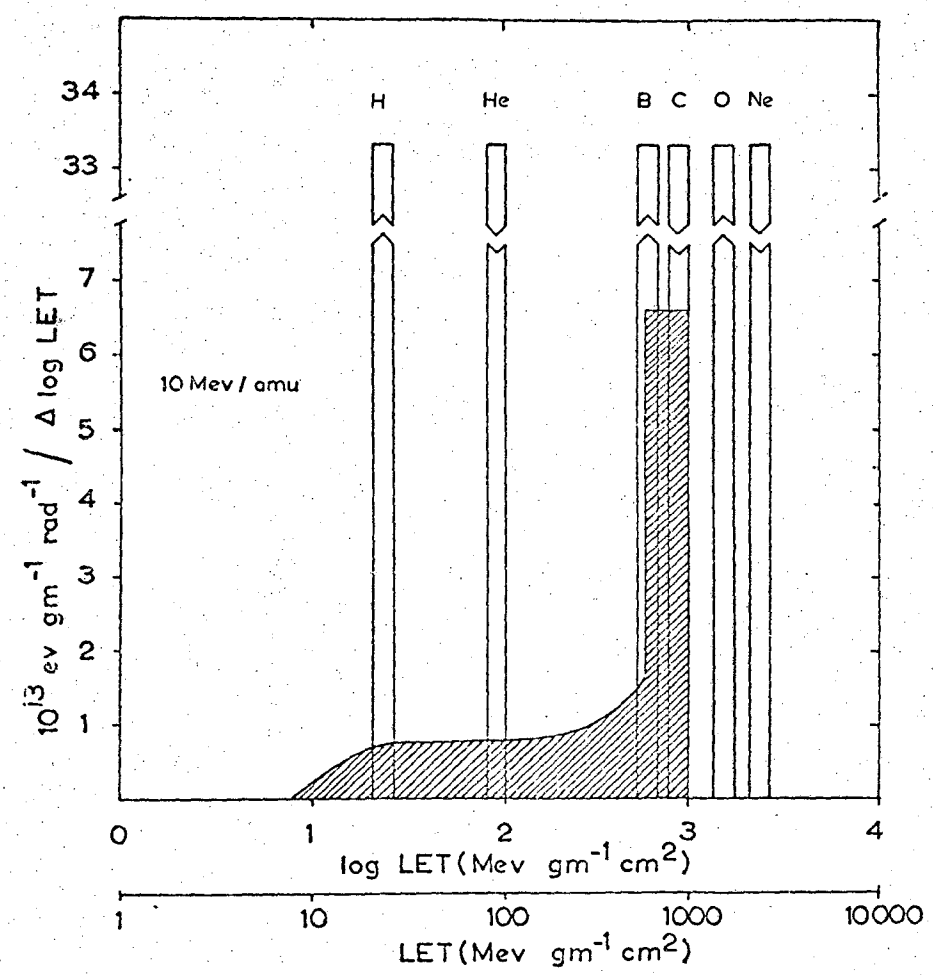
H
He
B C O Ne
34
33
7
6
5
4
3
2
1
10 Mev / amu
10^{13} ev gm^{-1} rad^{-1} / Δ log LET
0
1
2
3
4
log LET (Mev gm^{-1} cm^2)
1
10
100
1000
10000
LET (Mev gm^{-1} cm^2)

Fig. 9

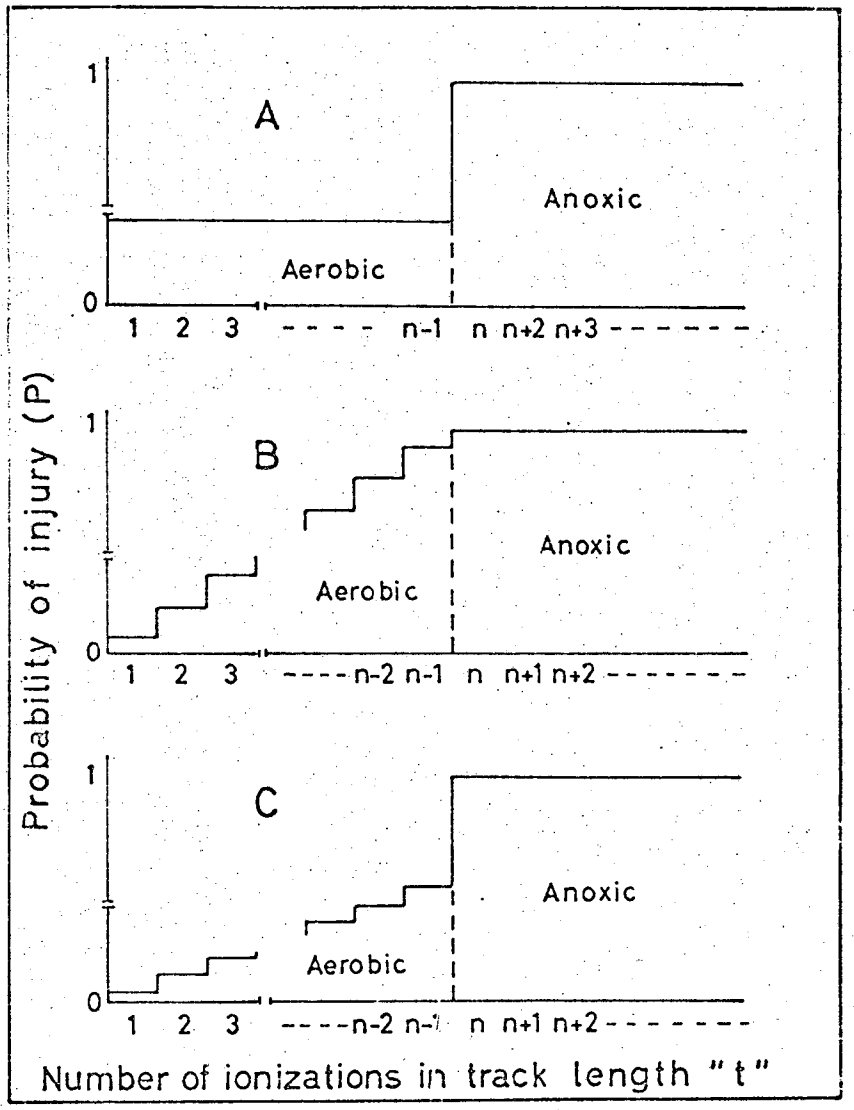
A
B
C
Anoxic
Aerobic
Probability of injury (P)
1
0
1 2 3 - - - - n-1 n n+2 n+3 - - - - - -
1 2 3 - - - - n-2 n-1 n n+1 n+2 - - - - - -
Number of ionizations in track length "t"

Fig. 10

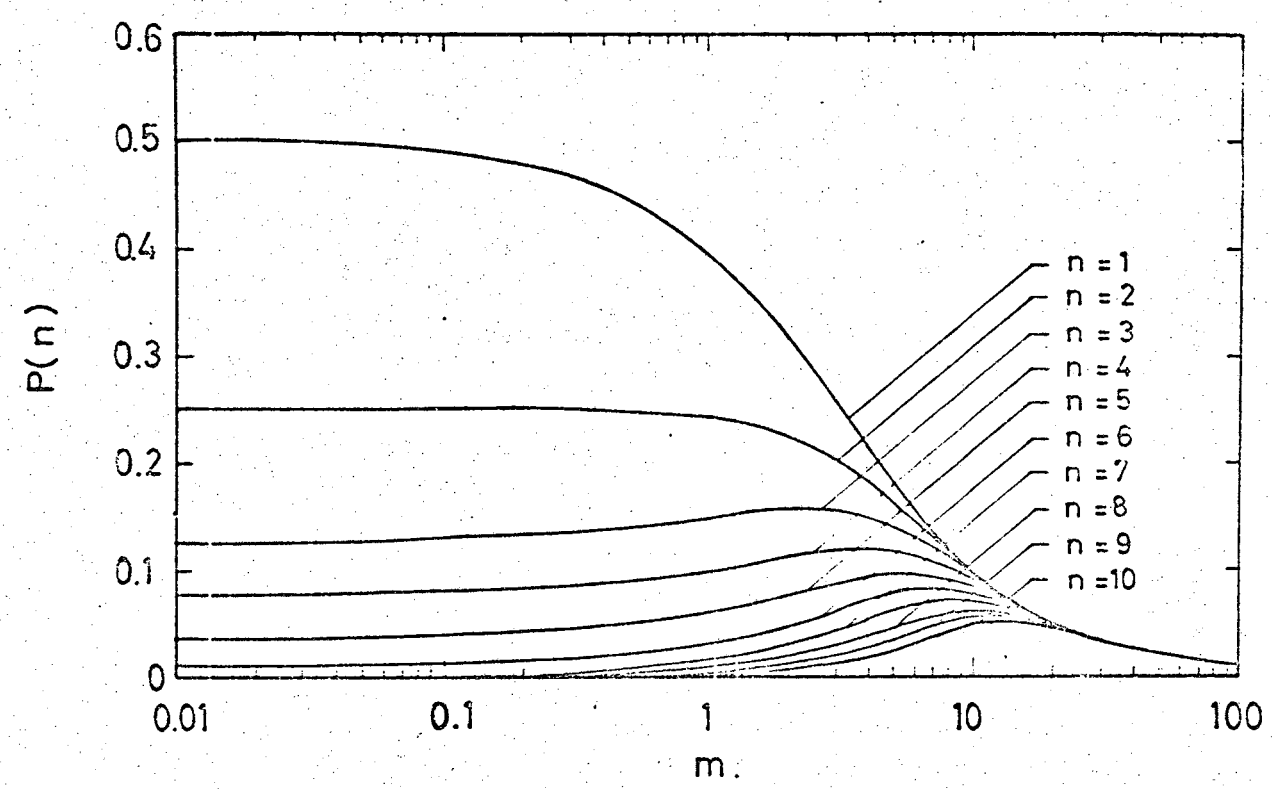

Fig. 11

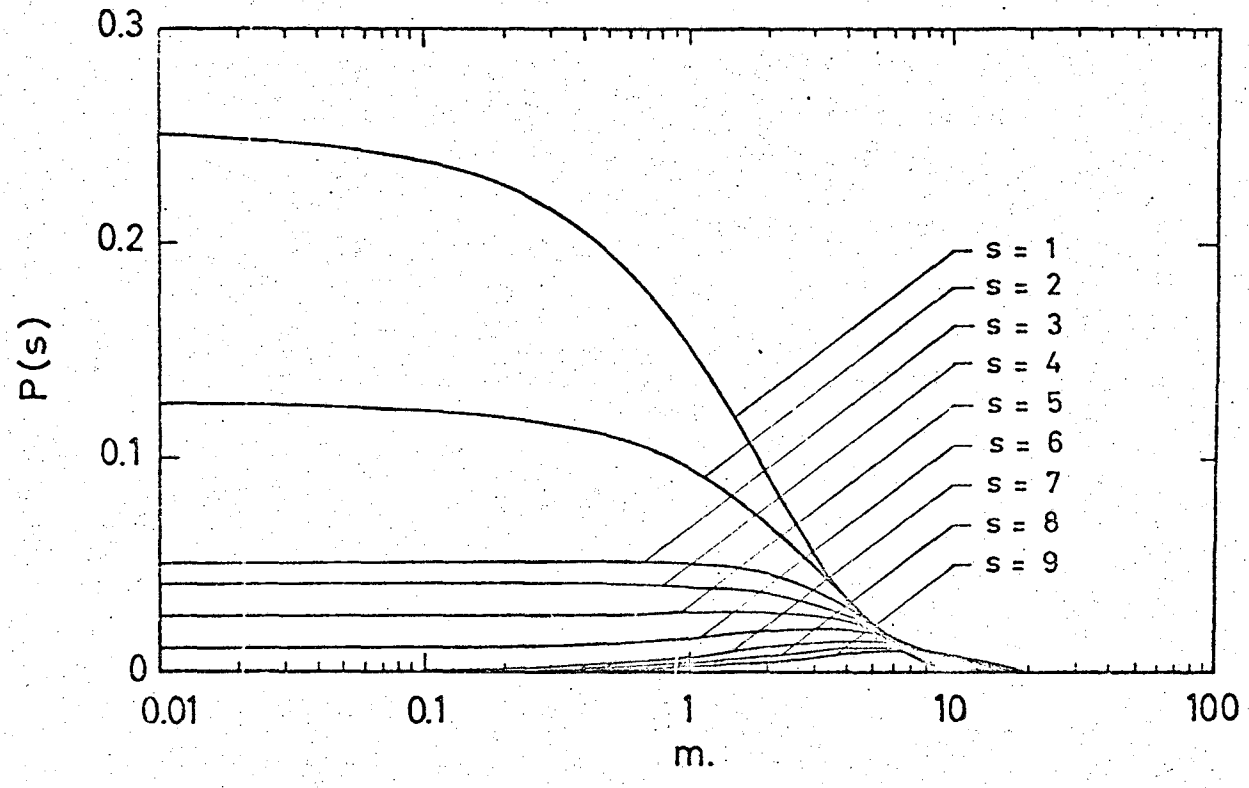

Fig. 12

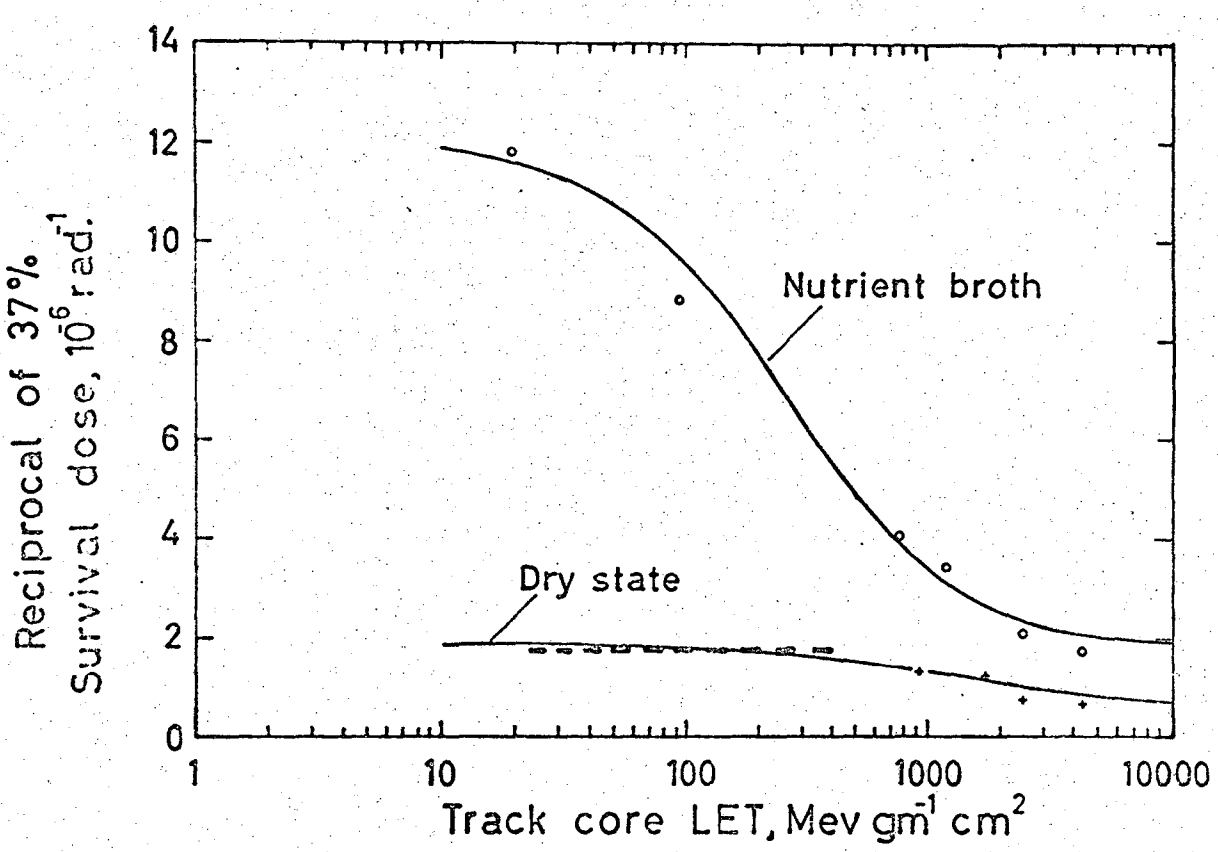
Reciprocal of 37% Survival dose, 10^{-6} rad.$^{-1}$
14
12
10
8
6
4
2
0
Nutrient broth
Dry state
1
10
100
1000
10000
Track core LET, Mev gm^{-1} cm^{2}

Fig. 13

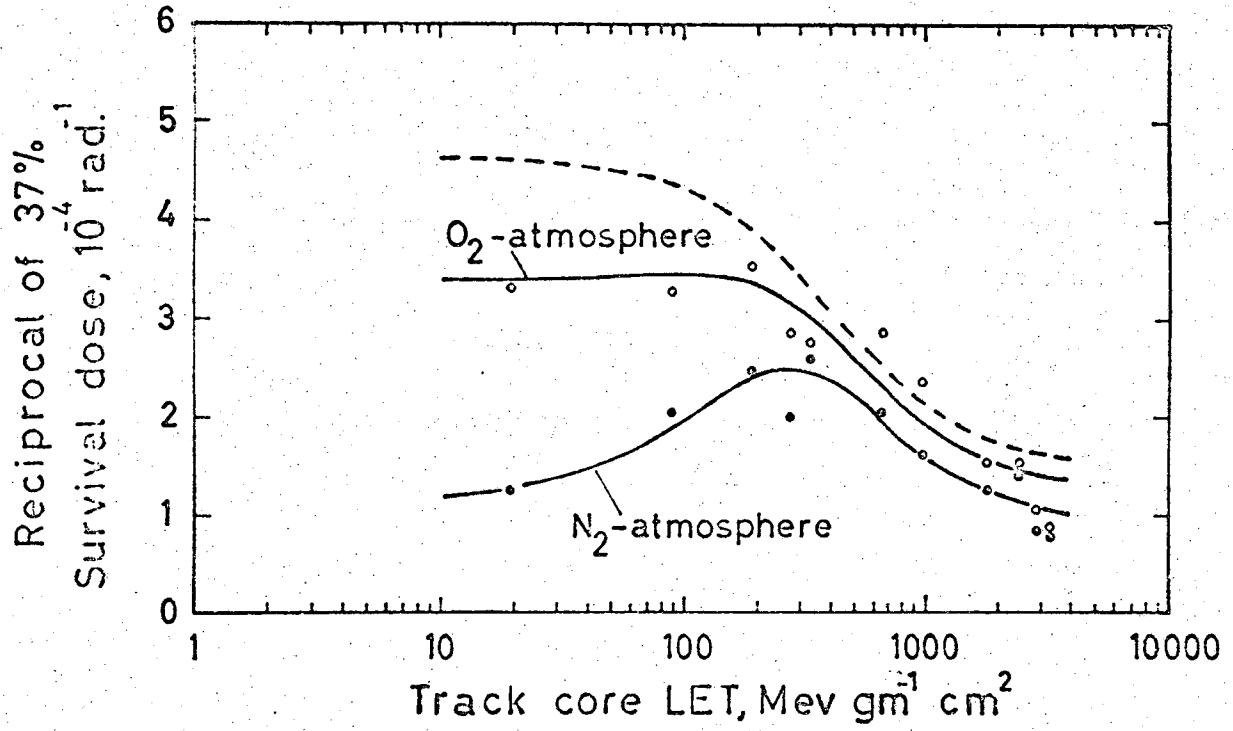
Reciprocal of 37% Survival dose, 10^{-4} rad.$^{-1}$
O_2-atmosphere
N_2-atmosphere
Track core LET, Mev gm^{-1} cm^2
0
1
2
3
4
5
6
1
10
100
1000
10000

Fig. 14

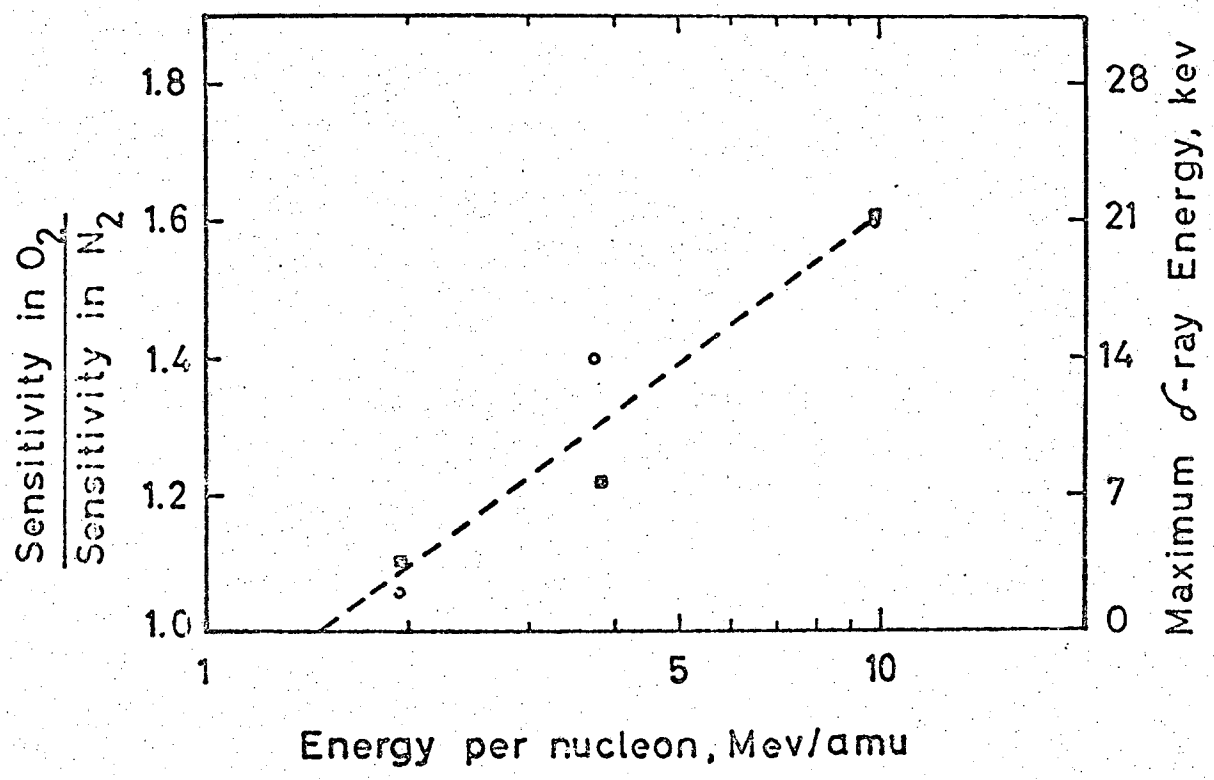
Sensitivity in O_2 / Sensitivity in N_2
1.8
1.6
1.4
1.2
1.0
1
5
10
Energy per nucleon, Mev/amu
28
21
14
7
0
Maximum δ-ray Energy, kev

Fig. 15

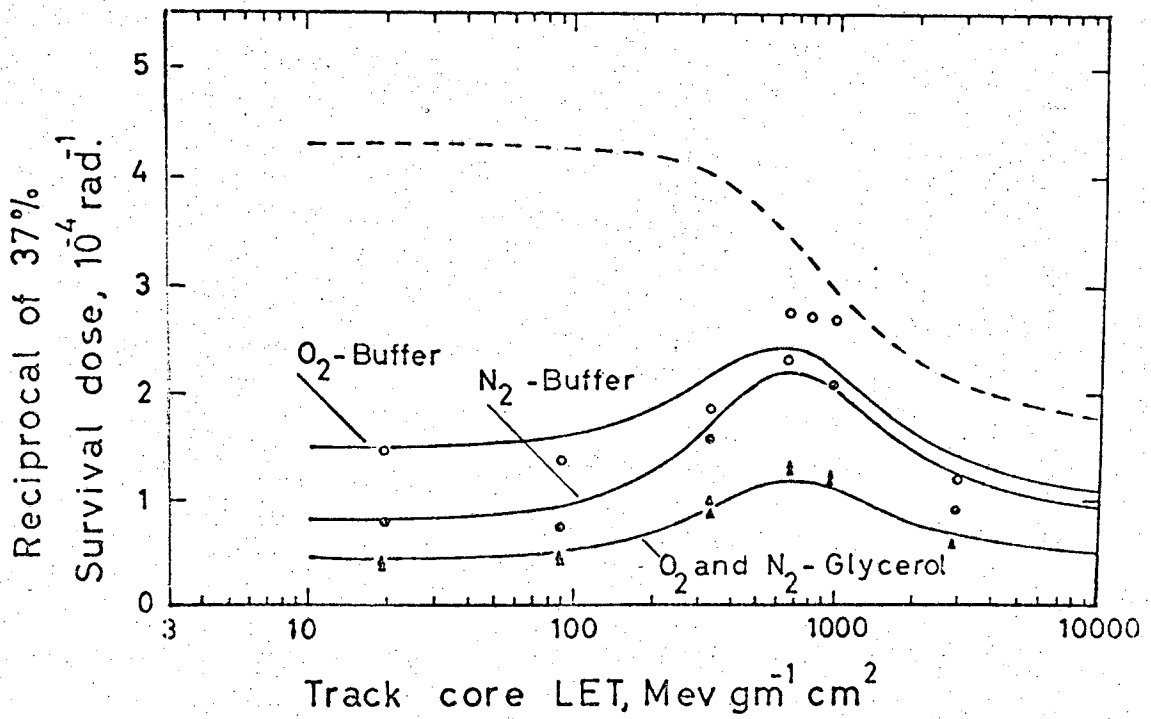
Reciprocal of 37% Survival dose, 10^{-4} rad.$^{-1}$
O_2-Buffer
N_2-Buffer
O_2 and N_2-Glycerol
0
1
2
3
4
5
3
10
100
1000
10000
Track core LET, Mev gm^{-1} cm^2

Fig. 16

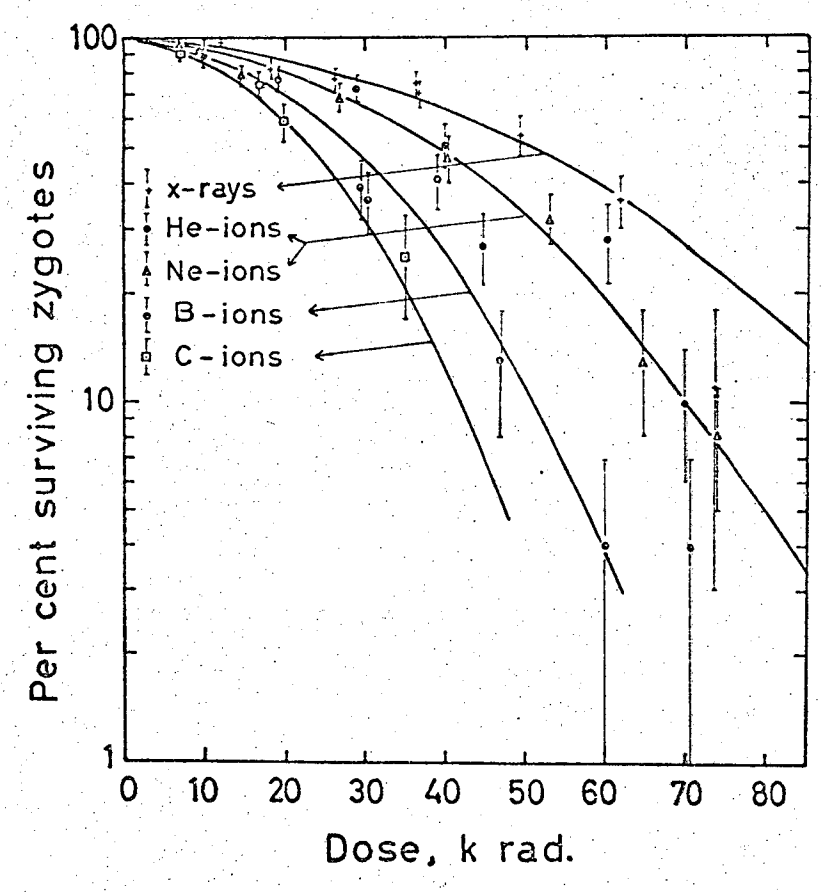
100
10
1
Per cent surviving zygotes
x-rays
He-ions
Ne-ions
B-ions
C-ions
0
10
20
30
40
50
60
70
80
Dose, k rad.

Fig. 17

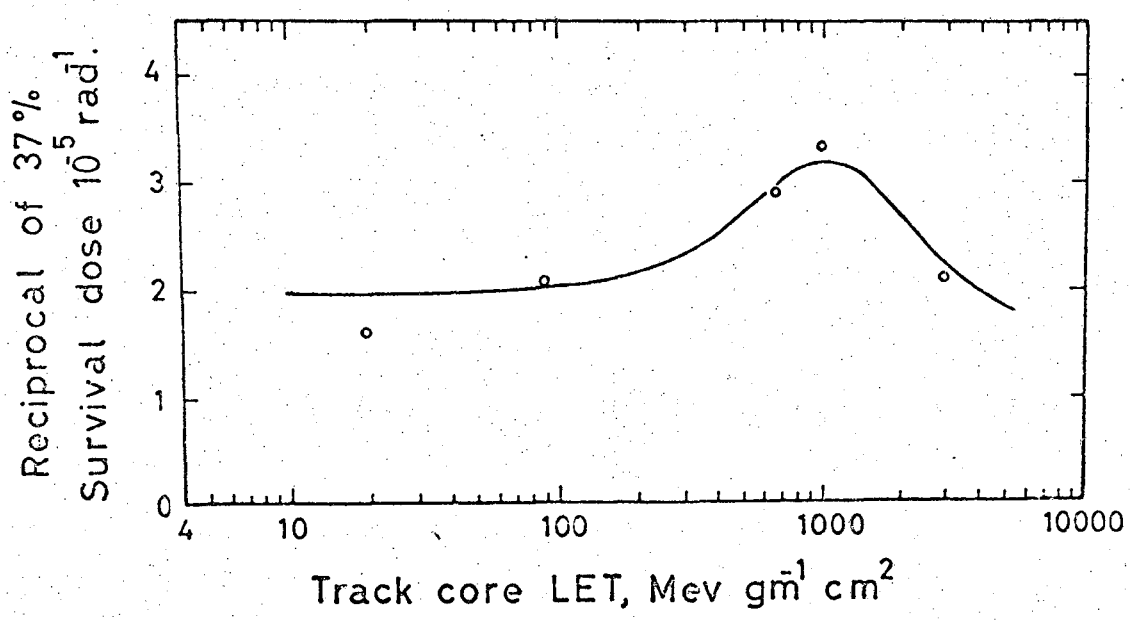
Reciprocal of 37 %
Survival dose 10^{-5} rad^{-1}.
0
1
2
3
4
4
10
100
1000
10000
Track core LET, Mev gm^{-1} cm^{2}

Fig. 18

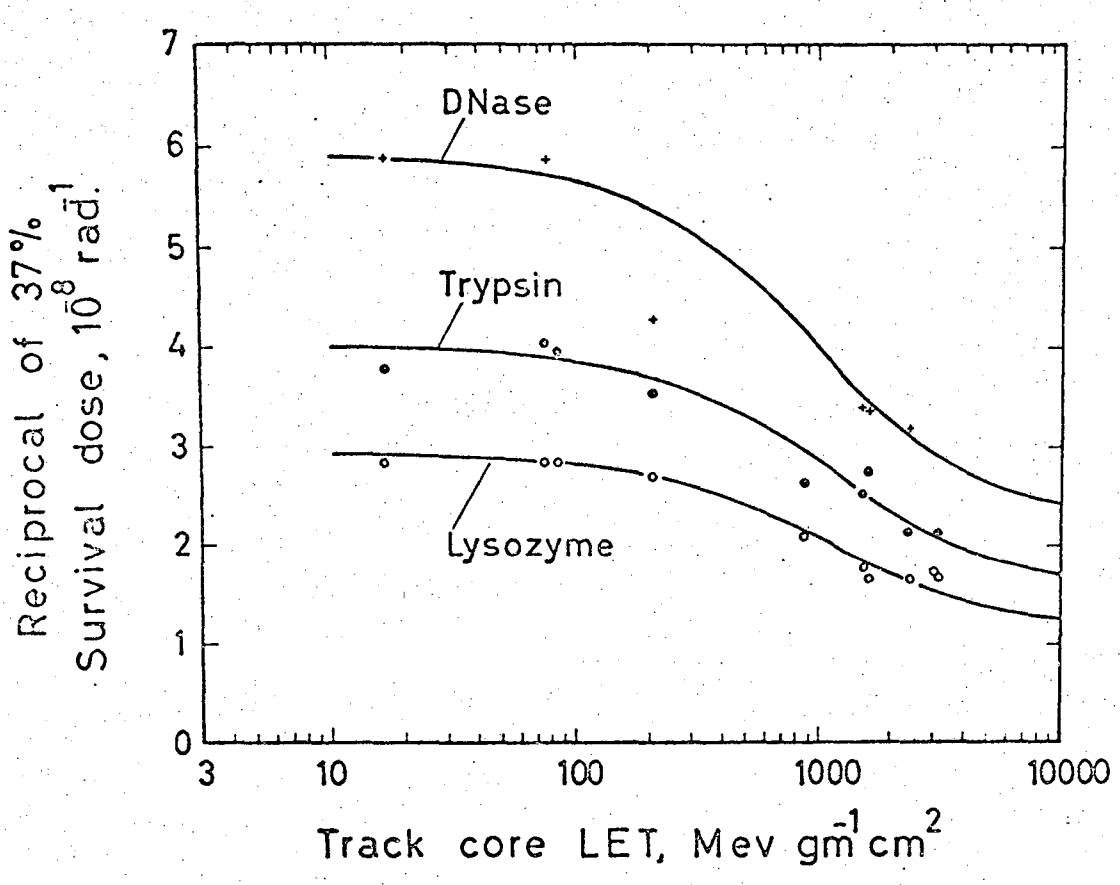
DNase
Trypsin
Lysozyme
Reciprocal of 37% Survival dose, 10^{-8} rad^{-1}
Track core LET, Mev gm^{-1}cm^{2}
0
1
2
3
4
5
6
7
3
10
100
1000
10000

Fig. 19

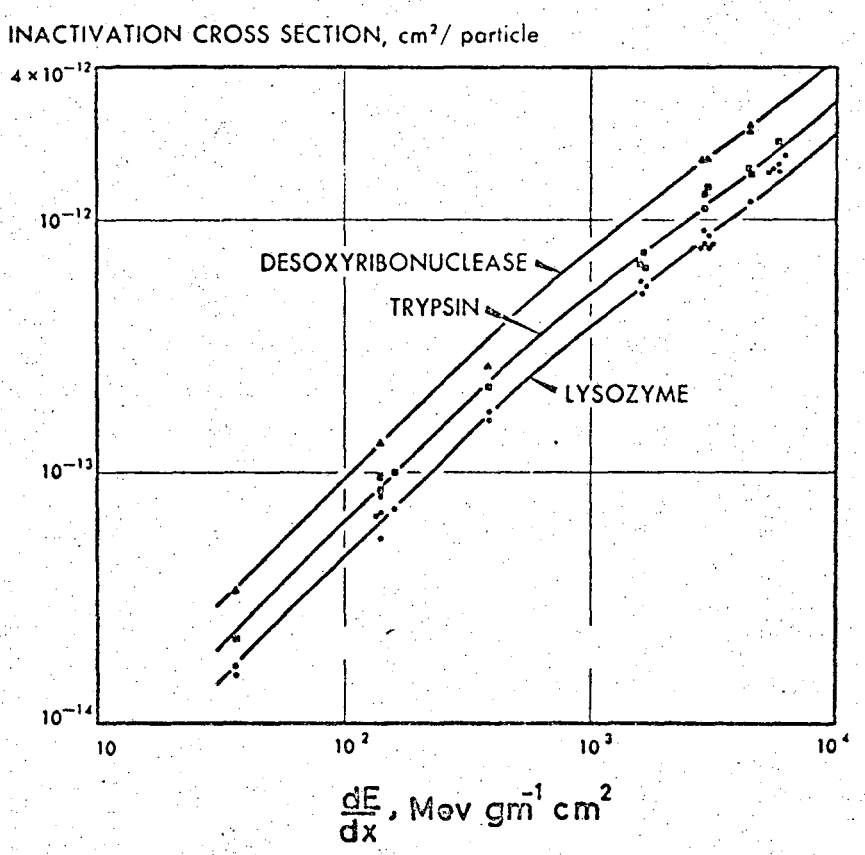
INACTIVATION CROSS SECTION, cm²/ particle
4 × 10⁻¹²
10⁻¹²
10⁻¹³
10⁻¹⁴
DESOXYRIBONUCLEASE
TRYPSIN
LYSOZYME
10
10²
10³
10⁴
dE/dx, Mev gm⁻¹ cm²

Fig. 20

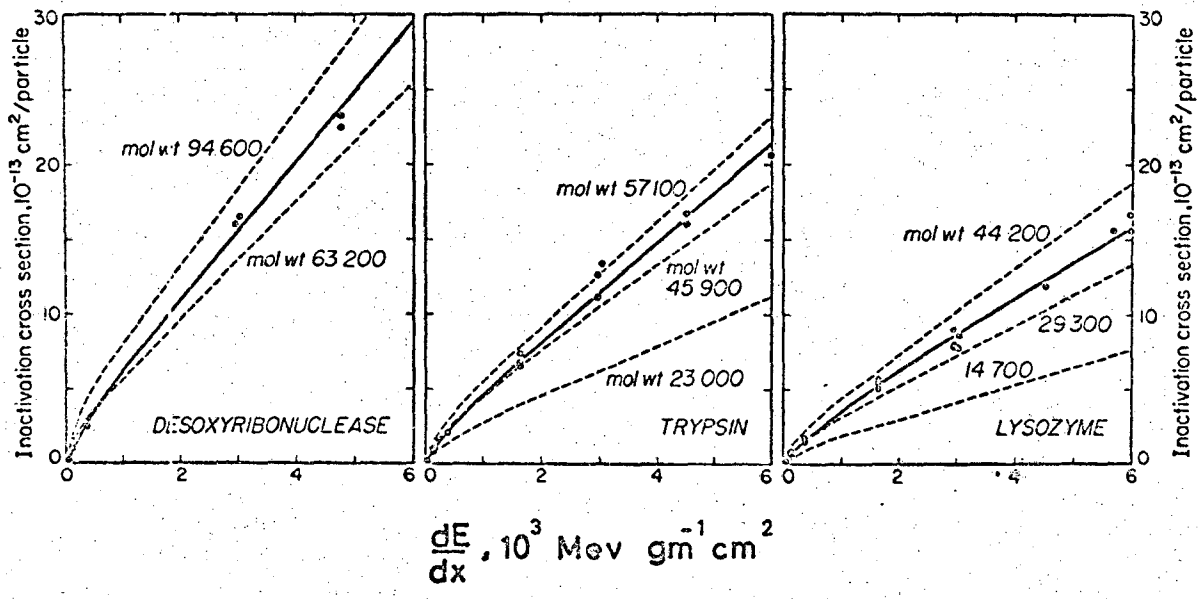
Inactivation cross section, 10^{-13} cm^2/particle
mol wt 94 600
mol wt 63 200
DESOXYRIBONUCLEASE
mol wt 57100
mol wt 45 900
mol wt 23 000
TRYPSIN
mol wt 44 200
29 300
14 700
LYSOZYME
$\frac{dE}{dx}$, 10^3 Mev gm^{-1} cm^2

Fig. 21

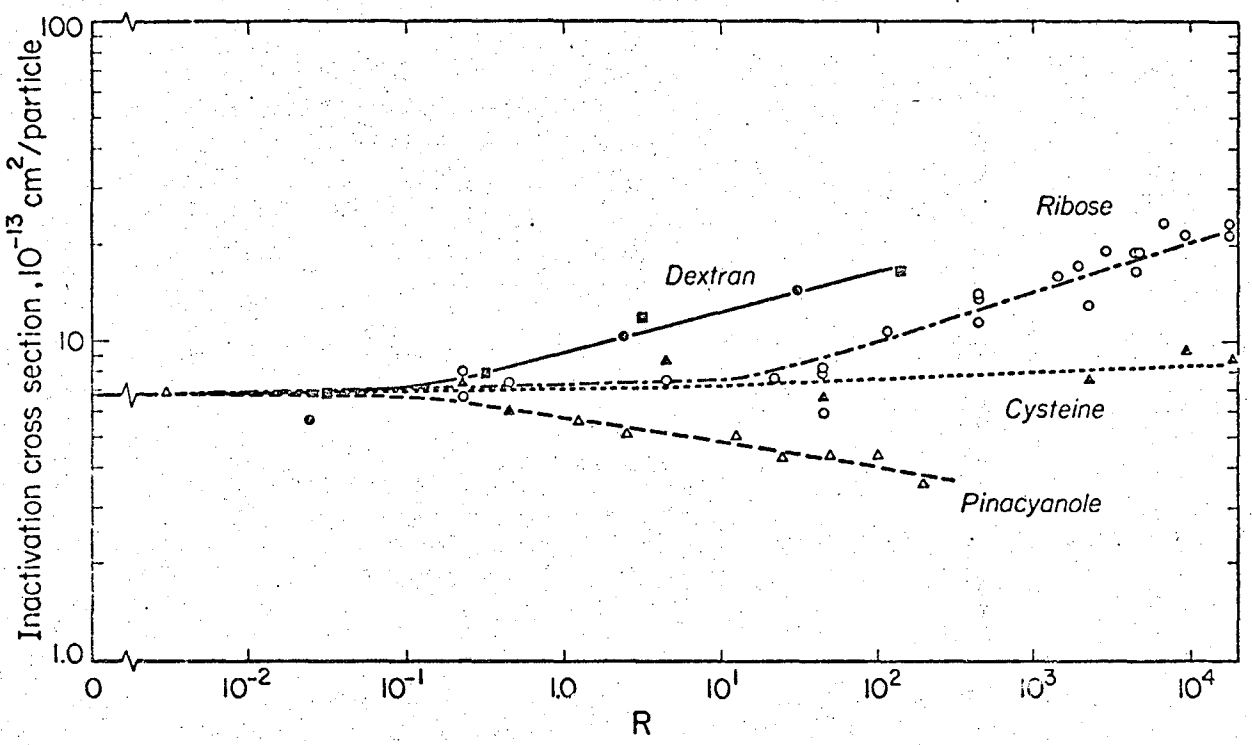
Inactivation cross section, 10^{-13} cm^2/particle
100
10
1.0
0
10^{-2}
10^{-1}
1.0
10^{1}
10^{2}
10^{3}
10^{4}
R
Dextran
Ribose
Cysteine
Pinacyanole

Fig. 22

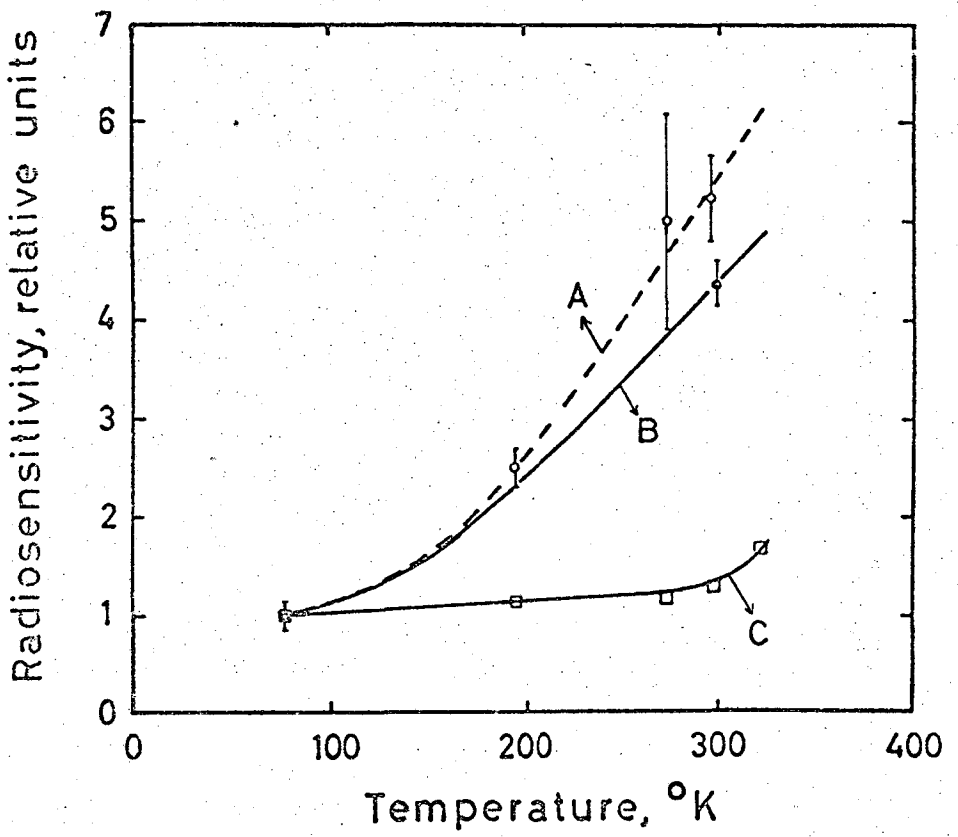
Radiosensitivity, relative units
0
1
2
3
4
5
6
7
0
100
200
300
400
Temperature, °K
A
B
C

Fig. 23